ESTIMATING GLOBAL CARBON TRENDS

USING IN-SITU pCO_2 OBSERVATIONS

By Amanda R. Fay

A thesis submitted in partial fulfillment

of the requirements for the degree of

Masters of Science

Atmospheric and Oceanic Sciences

at the

University of Wisconsin – Madison

December 2010

ESTIMATING GLOBAL CARBON TRENDS USING IN-SITU pCO_2 OBSERVATIONS

Amanda R. Fay

Under the supervision of Dr. Galen A. McKinley

ABSTRACT

While nearly half of total CO_2 emissions over the last 50 years remain in the atmosphere, this fraction is subject to large year-to-year variability due to erratic land and ocean sink rates (Le Quéré et al. 2009). In order to investigate the tendency for oceanic CO_2 uptake around the globe, long-term trends must be determined from available historical data. Recent studies of the North Atlantic carbon cycle, for example, suggest conflicting air-to-sea flux trends: data-based extrapolations report a declining sink (Schuster et al 2009), while models have suggested an increasing air-sea flux (Ullman et al. 2009). Likewise, significant debate is ongoing regarding the Southern Ocean carbon sink (Le Quéré et al. 2009; Boning et al. 2008; Ho et al. 2010). In order to resolve this carbon uptake debate, further analysis and direct model-data comparisons are needed.

This study uses a vast, newly updated, in-situ pCO_2 dataset (Takahashi et al. 2010) to analyze trends in the global ocean carbon sink over recent decades. We use two global biogeochemical models (Doney et al. 2009; Dunne et al. 2005) to evaluate methodologies for determining uptake trends in global timeseries

constrained by limited spatial and temporal coverage. Using a robust methodology within large, physical-biogeochemical defined regions or “biomes”, we diagnose surface ocean pCO_2 trends on decadal and multi-decadal timescales, along with the dominant mechanism of change: chemistry (pCO_2-nonT) or temperature (pCO_2-T). Comparison of these trends to the global atmospheric CO_2 trend provides us with insight in determining the future of the oceanic carbon sink in various regions of the world.

ACKNOWLEDGEMENTS

First and foremost I would like to thank my advisor, Dr. Galen McKinley, for allowing me to join her research group and for her expertise, encouragement, and support. She is an admirable scientists and a wonderful role model. I have thoroughly enjoyed working with her over the past few years and could not have completed this project without her guidance.

To my thesis readers, Dr. Ankur Desai and Dr. Dan Vimont, thank you for taking time out of your busy schedules to give me feedback .

I would also like to thank the entire McKinley research group, especially my officemate Val Bennington- your Matlab skills saved me years of work and your stories kept me entertained during long hours at my desk.

Many thanks to the AOS professors and my fellow graduate students who make this such a great department. Most importantly I would like to thank my fellow students in the incoming class of 2008, without whom I never would have survived my first year here, let alone made it to graduation. Thanks for teaching me that candy and baked goods can help you endure any late night or weekend homework session.

Finally, to my mom, who read countless drafts of posters and abstracts despite only understanding about half of the words, I owe you more thank-yous then I could possibly say in a lifetime. And to my sister Jessica who always welcomed me to Chicago whenever I needed to escape the stresses of school- I am forever grateful. A final thanks to my Oregon friends- I would not have survived Madison without your visits and your help keeping things in perspective.

TABLE OF CONTENTS

1. INTRODUCTION

Atmospheric carbon dioxide levels have increased dramatically since the Industrial Revolution with concentrations now exceeding 380ppm- levels over 30% higher than pre-1850 concentrations (Sarmiento and Gruber 2002). This change is primarily due to human activities, such as the burning of fossil fuels, cement production, and land use changes (Keeling and Whorf 2005). On average, only 43% of the emitted carbon dioxide has remained in the atmosphere (Le Quéré et al. 2009). The remaining portion is divided nearly equally between the two available carbon sinks: the terrestrial biosphere and the oceans (Sarmiento and Gruber 2002). This sink fraction is subject to large year-to-year variability and estimates show the fraction remaining in the atmosphere has increased by 0.3 ± 0.2% each year. Studies suggest that this trend in the atmospheric fraction of total emissions implies that the growth rate of carbon uptake by the world's CO_2 sinks is not keeping up with the increase in CO_2 emissions (Canadell et al. 2007). While multiple explanations have been proposed to explain this trend, the future behavior of these sinks remains uncertain. Further understanding of the behaviors of the world's carbon sinks is essential to understanding the potential future carbon dioxide levels in our atmosphere.

Changing land-use practices and biomass burning are impacting the terrestrial carbon sink, leading to a weak terrestrial sink on the order of 0.5 Pg C/yr (Friedlingstein et al. 2006). This leaves the oceans to serve as the primary long-term sink for anthropogenic carbon. Without the oceans ability to

remove carbon from the atmosphere, our climate would be dramatically different than it is today (e.g., Sabine et al. (2004) suggest that atmospheric CO_2 concentrations would be 55ppm higher than present levels).

Observations suggest that in some ocean regions, the carbon cycle is responding to climate variability and climate change in a way that could possibly affect the net uptake of CO_2 by the oceans (Takahashi et al. 2009). This thesis focuses on analysis of the partial pressure of CO_2 in surface waters ($pCO_2^{s.ocean}$), which serves as the dominant control of the ocean's carbon uptake. If the rate of change in the $pCO_2^{s.ocean}$ trend is faster (slower) than the rate of increase in the atmosphere on a comparable timescale, then the ocean carbon sink is declining (increasing). If the rate of change of $pCO_2^{s.ocean}$ is indistinguishable from the atmosphere given each trend's corresponding uncertainties, then this suggests a steady carbon sink.

This thesis aims to determine the trends in ocean carbon sink over various regions of the global ocean as well as the driving mechanisms of such trends. While regional studies suggest increasing or declining sinks (Takahashi et al. 2006, Schuster et al. 2009), recent estimates of the global ocean carbon sink trend predicts a trend comparable to the increase seen in the atmosphere, except with a slight lag due to slower mixing and gas exchange processes of the ocean (Le Quéré et al. 2010). Our analysis is accomplished by analyzing global surface ocean observations of pCO_2 using a methodology including both a harmonic and linear fit to in situ data. I establish the robustness of our methodology by utilizing two different physical-biogeochemical models to

determine trends from sparse data over large regions of the ocean. The ability of our methodology to capture the actual trends in $pCO_2^{s.ocean}$ is indicated by the fact that when I sample the model output as the data, I am able to recover the trends calculated from all model output within 1σ uncertainty bounds for a majority of the biomes.

2. DATA

i. Datasets

Database of surface ocean pCO_2 ($pCO_2^{s.ocean}$)

Direct global $pCO_2^{s.ocean}$ measurements (Takahashi et al. 2010) made using air- seawater equilibration methods (downloaded June 2010 from http://cdiac.ornl.gov/ oceans/LDEO_Underway_Database/index.html) are used for this analysis. Observations were collected by both international research groups as well as volunteer observing ships equipped with analysis equipment. The data covers a majority of the world ocean but is biased spatially with a majority of the data collected in the northern hemisphere (Figure 1,2). Dr. Taro Takahashi, at Lamont-Doherty Earth Observatory of Columbia University, is responsible for compiling the observations and initial quality control measures which are based on the stability of the system performance, the reliability of calibrations for CO_2 analysis, and the internal consistency of the data (Takahashi et al. 2010).

Partial pressure of CO_2 ($pCO_2^{s.ocean}$) levels in the global oceans are obtained from surface water samples using a turbulent water-air equilibration method. The turbulent water-air equilibration method, as described in Takahashi et al. 1993, involves equilibrating a volume of carrier gas with seawater, then measuring the concentration of CO_2 in the equilibrated carrier gas using a CO_2 gas analyzer (either by infrared CO_2 absorption or gas chromatographic analyses). Next, pCO_2 of the seawater is computed at an equilibrium

temperature using the relationship between the mole fraction of CO_2 in dry air and the pressure difference between the carrier gas in the equilibrium chamber and the water vapor pressure:

$$pCO_2 = (CO_2\ conc.)_{air} \bullet (P_b - P_w)$$

where P_b is the pressure in the chamber containing the carrier gas and P_w is the equilibrium water vapor pressure. A constant-chemistry temperature effect equation (Takahashi et al.1993) is used to correct back to the in situ seawater temperature. The corrected in situ pCO_2 observations at observed temperatures are used for this study. The average precision of the obtained pCO_2 measurements is estimated to be ± 2.5μatm.

Initially, all global observations (4,737,324 observations) were included for this analysis of open ocean carbon trends. However, coastal influences were found to be an influence and thus were eliminated by excluding data with reported sea surface salinity (SSS) values of less than or equal to 20psu. After this elimination, 327,000 of the remaining data points fell outside of our defined biomes (see Biomes section for details). Upon plotting these data points on a global map we found that a majority of them lie in coastal waters (areas not covered by SeaWiFS chlorophyll climatology) and for this reason are not captured in our regions of analysis (Figure 3). These points were eliminated from further analysis, as our focus is the open ocean. Coastal ocean waters lie at the interface between the terrestrial and ocean carbon systems. While these regions are important to consider when estimating global carbon flux (land and ocean), they represent only a small fraction of the global ocean and contain complex

physical and biological factors that are not considered in this analysis.

Data collected during El Nino events is retained in our dataset even though this was eliminated in the creation of the climatological pCO_2 (Takahashi et al. 1993, 2002, 2009). A total of 4,340,555 points are used in our global analysis, spanning years 1957 thru 2010.

SURATLANT

Data were collected along ship tracks between Iceland and Newfoundland (Corbiere et al. 2007; Metzl et al. 2009). SURATLANT $pCO_2^{s.ocean}$ is calculated from measurements of DIC, SST, SSS, and ALK using accepted constants (Mehrbach et al. 1973; Dickson 1990), and spanning years 1993-1997 and 2001-2007. We used the collected open-ocean data in the region of 50-64°N, 25-50°W Schuster et al. 2009). For 2001- 2007, ALK was directly measured, while for 1993-1997, ALK was estimated from the ALK- SSS relationship derived from 2001-2006 data (ALK = 43.857 * SSS + 773.8).

Because $pCO_2^{s.ocean}$ values are calculated versus being measured in situ, as with the Takahashi database, we conducted the analysis both with and without these observations. The absolute magnitudes of the trends shift slightly but mechanistic control interpretations do not change. We include these observations as they serve to fill a gap in subpolar North Atlantic in 2001-2002.

Climatologies

The revised version (June 2009) of climatological mean $pCO_2^{s.ocean}$ at 4° (latitude) x 5° (longitude) resolution for reference year 2000 (Takahashi et al.

2009) is used and regridded to 1°x1° resolution for our analysis. This climatology is used in step (ii) of the trend estimation (see Methodology section) in order to eliminate any potential spatial aliasing caused by the large areas of interest.

Trend in atmospheric pCO_2 (pCO_2^{atm})

The trend in pCO_2^{atm} is the mean of the annual growth rate based on globally averaged marine surface data from NOAA ESRL (http://www.esrl.noaa.gov/gmd/ ccgg/trends/) during 1981-2009 (1.66±0.07 ppm/yr) and for 1981-1995 (1.45±0.07 ppm/yr). For comparison, trend estimates from Mauna Loa spanning 1981-2009 produced a similar value (1.69±0.11 ppm/yr), while the trend for the longest record available (Mauna Loa 1959-2009) produced a slightly lower average (1.42±0.11 ppm/yr). The impact of time trends in atmospheric pressure on pCO_2 is very small and therefore is neglected in this analysis, allowing ppm/yr and µatm/yr to be used interchangeably. Global averages in atmospheric trends reported in µatm/yr are used in this analysis.

ii. Biome Selection

Data are scarce (Takahashi et al. 2009) yet the ocean carbon sink operates across the vast global oceans. Analysis of ocean uptake trends over small, latitudinally defined regions may not supply globally relevant information about the state of the global carbon cycle. In order to make the best use of the data, I estimate trends over physical-biologically defined biogeographic regions or "biomes" (Figure 4, Table 1). The criteria for these regions are based on those

used by Sarmiento et al. (2004), except without vertical velocity constraints as included in their analysis. Despite this difference, the biome boundaries are comparable between this study and those from Sarmiento et al. 2004. Such large biomes allow calculation of ocean carbon sink trends on the basin-scale, which provides evidence of the ocean's impact on the global carbon budget.

Global biome assignments are based on three criteria: maximum mixed layer depth (MLD), chlorophyll-a (Chl), and sea surface temperature (SST). A list of the different biomes, together with the criteria used to define them, is presented in Table 1.

For the climatological biomes, annual MLD values were calculated from World Ocean Atlas outputs using a surface to depth density difference of 0.125 kg/m^3 (Antonov et al. 2006). Due to insufficient coverage in the climatology, especially in the southern hemisphere, grid cells missing max MLD values were assigned the latitudinal mean. Annual mean chlorophyll-a was taken from SeaWiFS, averaged over years 1998 to 2008, while climatalogical SST was averaged over 1982-2007 (Reynolds & Smith 1994). All parameters are gridded to 1°x1° resolution.

Biome	Chl (mg/m^3)	SST (°C)	MLD (m)
NH Marginal Sea Ice (ICE)		< 4	
NH Subpolar (SUB)	≥ 0.45	< 15	
NH Seasonally Stratified Subtropical (SES)	< 0.45	< 24	> 150
NH Permanently Stratified Subtropical (PSS)	< 0.45	≥ 9	≤ 150
Equatorial (EQU)		≥ 9	
SH Permanently Stratified Subtropical (PSS)	< 0.45	≥ 15	
SH Seasonally Stratified Subtropical (SES)	< 0.9	9 ≤ x < 19	
SH Subpolar (SUB)		< 9	
SH Marginal Sea Ice (ICE)		< 4	
Low Latitude Upwelling (LLU)	≥ 0.25		

Table 1: Criteria used to designate global biomes.

The fundamental differences between these biomes are the large-scale physical processes that control nutrient supply. Cooler waters that exhibit ice cover during some part of the year, are grouped into the marginal sea ice (ICE) biome, characterized by average temperatures below 4°C. Poleward of 30° latitude, the subpolar (SUB) biomes have divergent surface flow driven by the positive wind stress curl (i.e. upwelling), allowing for higher chlorophyll concentrations due to continual nutrient resupply. A seasonally mixed subtropical (SES) biome is an area of downwelling, due to the negative wind stress curl, but is characterized by intermediate chlorophyll concentrations due to deep winter MLDs that penetrate into the high-nutrient waters of the thermocline. The permanently stratified subtropical biome (PSS) is physically defined by a negative wind stress curl, which promotes convergence and stratification. This means MLDs are shallow and Chl is low (i.e. an area that is nutrient limited), thus classifying it as oligotrophic.

Around the same latitude band as the global subtropical gyres there are regions of upwelling, predominantly on the western coastlines of continents, which have high biological productivity due to high nutrient supply. These regions are put into their own classification of global low-latitude upwelling regions (LLU). Equatorially biomes (EQU) are defined as covering the latitude band between 5°S and 5°N where warm waters, strong equatorial upwelling, and high levels of downwelling radiation are dominant factors in determining where high biological productivity occurs. This definition of the EQU biome varies however in the Indian Ocean where the equatorial region is grouped in with the PSS biome due to seasonally varying physical ocean circulation patterns linked to the monsoon.

Biomes were also separately assigned for the two models employed in our analysis. For each model, corresponding model SST, max MLD, and surface chlorophyll output were used to classify the biomes.

The same selection criteria were used for both climatological and model biomes except for a change in the chlorophyll criteria in the northern hemisphere SUB biome. In this biome, the MOM model has chlorophyll criteria of ≥0.25mg/m^3 while the CCSM3 model chlorophyll criteria is ≥0.15mg/m^3 (as compared to ≥0.45mg/m^3 in the climatological biome). This modification in biome selection criteria was required due to consistently low reported chlorophyll levels in model output (Bennington et al. 2009; Doney et al. 2009). The resulting biomes for each model and from the climatologies are similar (Figure 5a,b).

iii. Global physical-biogeochemical models

Two global models are employed in this project: the Community Climate System Model (CCSM-3) ocean carbon model and GFDL's MOM-TOPAZ global ocean model.

The CCSM-3 model is a global, three-dimensional ocean general circulation model which runs from 1958-2009 at a spatial scale of 3.6° longitude x 0.6°-1.5° latitude. The model is forced with physical climate forcing from atmospheric reanalysis as well as satellite data products. It also contains time-varying atmospheric dust deposition.

CCSM-3 incorporates a multi-phytoplankton functional group ecosystem module with multi-nutrient limitation on phytoplankton growth (Doney et al 2009). Model-data skill assessments as described by Doney et al. (2009) show a bias in surface chlorophyll levels (model values tend to be too high in the subtropical oligotrophic gyres and too low in the subpolar gyres). This results in the model's underrepresentation of the magnitude of the peak northern hemisphere summer surface chlorophyll concentrations due to its inability to sustain the spring bloom. Comparisons between zonally averaged SST model output and data shows strong correlation in all ocean regions, whereas model-data comparisons of ΔpCO_2 show good correlation in the Pacific Ocean, however the model has difficulty capturing the data in the Atlantic Ocean, especially in the equatorial region (model underestimates ΔpCO_2) and midlatitudes (underestimates ΔpCO_2 in the southern hemisphere and over estimates ΔpCO_2 in the northern hemisphere). Comparison of seasonal climatologies for SST and pCO_2 yield

small global mean biases.

The MOM-TOPAZ model is a global biogeochemical and ocean ecosystem model which runs from 1959-2004 at a spatial resolution of nominally 1°, with higher latitudinal resolution near the equator, reaching as small as 1/3°. The model is forced with the CORE reanalysis dataset, which is based on the NCEP forcing with additional satellite data incorporated (Henson et al. 2010). The biogeochemical model contains all major nutrients and three classes of phytoplankton with growth rates co-limited by nutrients and light (Henson et al. 2010) along with dust deposition fluxes prescribed from monthly climatology (Ginoux et al. 2001). Drifting of midlatitude westerlies in this model contributes to a cold bias associated with an equatorward contraction of the oceanic subtropical gyre circulations (Delworth et al. 2006). Additionally, the MOM-TOPAZ model has difficulty capturing the 10-year mean SeaWiFS chlorophyll trend, overestimating the chlorophyll trend in the high latitude and oligotrophic regions in both the North Pacific and Atlantic Ocean basins.

3. METHODOLOGY

While nearly half of total CO_2 emissions each year remain in the atmosphere, this fraction is subject to large year-to-year variability. In order to investigate the tendency for oceanic CO_2 uptake around the globe, long-term trends must be determined from available historical data. By compensating for large spatial and temporal biases, biome-based regional $pCO_2^{s.ocean}$ trend estimates, along with corresponding 1σ uncertainties, are calculated. I experimented with a variety of trend estimation methods. First I will discuss my chosen methodology and then I will comment on alternatives that were eventually not selected.

i. Estimation of trends

To estimate trends in $pCO_2^{s.ocean}$ for each of the biomes, I use the following methodology:

i. Global data are gridded to 1° x 1° spatial and then averaged to monthly temporal resolution.
ii. The long-term annual mean for each 1° x 1° cell is removed to eliminate spatial aliasing before analyzing over large regions.
iii. Monthly anomalies are then averaged for each biome and ocean basin (resulting in 19 regions globally).
iv. A harmonic of the form $y = a + b*t + c*\cos(2\pi t + d)$, where t is the decimal year - 1957, is fit to capture both a sinusoidal annual cycle and a linear trend for the data in each biome. A harmonic analysis routine,

using the least-squares method, is used to fit coefficients a, b, c, and d. Trends reported in our analysis are the value of coefficient b (in μatm/yr) resulting from the fit (Figure 6).

A major source of error in estimating temporal trends from sparse ocean data arises from potential aliasing of differences in space because sampling points differ from year to year. Step (ii) of the methodology minimizes this spatial aliasing effect by subtracting out a long-term annual mean for each gridcell in the biomes. The ability of this methodology to capture the actual trends in $pCO_2^{s.ocean}$ is confirmed in the Model Confirmation portion of this section.

Trends are calculated beginning in 1981 as the bulk of available data (especially in previous releases of this dataset) are contained in the past thirty years. Additionally, robust trends were difficult to achieve when calculating trends over longer timescales as the sparse data caused large errorbars. Over 99% of the total in situ observations come from post 1981. When narrowing down the data to consider only monthly means by biome, an average of 90% of the monthly means falls during the years 1981-2010.

I have tested several analysis schemes with a numerical model that has high fidelity for the large-scale physics and carbon biogeochemistry of the global ocean and find that this methodology is optimal. I also estimated trends by deseasonalizing the $pCO_2^{s.ocean}$ using Takahashi's climatology (Takahashi et al. 2009) and applying a linear fit. Results for the biomes are indistinguishable from the use of the harmonic fit. Another method I investigated was a linear fit to

seasonal averages. Due to limited multi-year seasonal coverage in many of the biomes, yielding large uncertainty on the estimates this method was discarded. I elected to use the harmonic fit as my standard analysis approach so as to capture both a seasonal cycle and linear trend without requiring a climatology for the parameter of interest as this is not always available (DIC, ALK, etc).

Through a variety of trend estimation techniques, I have found that the use of spatially binned monthly data (as is used in Schuster et al. 2009), as opposed to spatially averaged monthly data, has the largest impact on differences in reported estimated trends. The spatially binned method includes all monthly mean values from grid cells (1°x1° in the analysis of Schuster et al. 2009) in the analysis while the spatially averaged monthly data method results in one average monthly mean for the entire biome, calculated from the mean of each gridcell's monthly mean. Binning the data gives much smaller 1σ confidence intervals because it suggests a higher N value and thus more degrees of freedom. With so many global data observations (over 4 million) the confidence intervals on trends calculated over such large biomes become meaningless and all trends become statistically significant.

ii. Trend uncertainty

I present the 1σ confidence intervals (68.3%) for the resulting $pCO_2^{s.ocean}$ trends, meaning that the true trend is expected, with 68.3% confidence, to lie within the reported interval. These intervals express a region that if repeated samples of the same size were drawn from the same population and confidence

bounds were defined for each, then 68.3% of these regions would include the true parameter (the true $pCO_2^{s.ocean}$ trend). The equation used for the confidence of the trend (b) is

$$CI = \pm t * RMSE * \sqrt{\frac{1}{\sum (x_i - \bar{x})^2}}$$

Where *t* is the two-tailed t-statistic for 68.3% confidence and N-4 degrees of freedom (N being the number of months containing an observation), *RMSE* is the root mean square error, x_i are the monthly mean anomalies obtained after processing via the methodology in Section 3 (i); and $\bar{x}$ is the mean value of the monthly mean anomalies (von Storch and Zwiers 2002).

iii. Model Confirmation

In order to verify our method of calculating the $pCO_2^{s.ocean}$ trend over biomes despite variable spatial and temporal data coverage, I have employed two physical-biogeochemical models. By sampling each model as the data and applying the same methodology as explained above to obtain a trend, I would ideally capture the $pCO_2^{s.ocean}$ trends calculated using all model output. Due to the shorter time span of the MOM-TOPAZ model run (ending in 2004), and the minimal observations available prior to 1980, I will be using the years 1981-2004 for this confirmation process.

When sampling the model as the data, we do so monthly at the model's spatial resolution and then treat the sampled model as the data, using the model climatology in step (ii) of the analysis. While only monthly resolution is available

for the global climate models used in this analysis, daily model output is available for the MIT-GCM, a North Atlantic global biogeochemical model (Ullman et al. 2009). A comparison of true model trends and sampled model trends using daily output versus monthly output from this model yielded similar values. This comparison suggests that monthly resolution of model output is sufficient for the confirmation technique employed in this analysis.

For this study, a biome will be considered "confirmed" if at least one of the two global climate models is able to capture the true model trend with the sampled model trend given 1σ uncertainty bounds (68.3%) on each estimate (Figure 7 a-f). For example, in Figure 7a, sampled model and true model trends are shown for each of the biomes in the North Pacific (distinguished by color for the different biomes and marker style for each of the models). Horizontal errorbars represent the uncertainty of the trend calculated using all model output, while vertical errorbars represent the confidence interval of the trend calculated from model output sampled as the data. If the intersection of the errorbars for a specific biome crosses the 1-1 line, the biome is considered "confirmed"- the sampled and true model trends are indistinguishable from one other given the uncertainty bounds.

Out of the 19 basin-divided global biomes, 8 have sampled trends confirmed by both models, 4 have their sampling verified by the MOM-TOPAZ model only, while 4 biomes are confirmed solely by the CCSM3 model (Figure 8, Table 2). The North Atlantic ICE and Southern Ocean ICE biomes are not confirmed by either model and will thus be eliminated from further trend analysis

in this study. This is likely due to the limited data available for these regions of the ocean as a result of difficult ocean conditions and ice-cover during portions of the year. The North Pacific ICE biome, while confirmed by both biomes, only contains three observations when using the climatological biome boundaries and thus a harmonic and linear trend cannot be defined (4 coefficients requires a minimum of 4 data points as inputs). Therefore it will also be eliminated from further analysis in this report, leaving 16 of the 19 biomes for further consideration.

Global area-weighted trends

A global area-weighted trend can be determined from the trends calculated for each biome. By multiplying the area of a biome by the $pCO_2^{s.ocean}$ trend for that biome and then taking the sum of the calculations and dividing by the total area of global oceans (contained in the biomes), an area-weighted trend is determined. Because not all of the global biomes are confirmed by the models I have calculated a global trend for all 19 biomes as well as a global trends including only the 16 confirmed biomes. The difference between these two trends is indistinguishable when considering confidence intervals.

Comparison to pCO_2^{atm} trends

The difference between the partial pressure of CO_2 in the surface ocean water and that of the overlying air determines the direction of the flux of carbon between the ocean and atmosphere. The difference in rates of increase between the ocean and atmosphere causes changes in the ocean carbon sink. The

carbon flux of the ocean is proportional to ΔpCO_2 where ΔpCO_2 is the difference between $pCO_2^{s.ocean}$ and pCO_2^{atm}. In the following equation,

$$FLUX = kw*rho*([CO_2]_{ocean} - [CO_2]_{atm})$$

kw is the gas transfer velocity, rho is seawater density, $[CO_2]_{ocean}$ is the surface ocean concentration of carbon dioxide, and $[CO_2]_{atm}$ is the saturation concentration of the atmosphere (Sarmiento and Gruber 2006). Note that pCO_2 directly determines CO_2 concentrations through water chemistry.

In biomes where the $pCO_2^{s.ocean}$ trend and corresponding error bars fall below the atmospheric trend the ocean carbon sink is said to be increasing as the oceanic carbon content is increasing at a slower rate than the atmospheric carbon. Likewise, in biomes where the $pCO_2^{s.ocean}$ trend and corresponding error bars lie above the atmospheric trend, the conclusion is a reported decline in the oceanic carbon sink as the carbon content of the surface ocean is increasing at a faster rate than that of the surrounding atmosphere.

iv. Decomposition of $pCO_2^{s.ocean}$

The CO_2 partial pressure in seawater (pCO_2) is a function of temperature (T), total CO_2 concentration (TCO_2), alkalinity (ALK), and salinity (SSS), following the thermodynamic relationship given by Takahashi (1993):

$$dpCO_2 = (\delta pCO_2/\delta T)\, dT + (\delta pCO_2/\delta TCO_2)\, dTCO_2 + (\delta pCO_2/\delta ALK)\, dALK + (\delta pCO_2/\delta SSS)\, dSSS$$

In this study, monthly mean $pCO_2^{s.ocean}$ for each biome is decomposed into two components: the isochemical component due to temperature (pCO_2-T) and

the remaining variability (pCO_2-nonT) assumed to be due to biological and chemical factors salinity SSS, ALK, and dissolved inorganic carbon (DIC) defined as the sum of the concentrations of all dissolved carbon species. This method of decomposition was developed by Takahashi et al. (2002) using the empirical equations:

$$pCO_2 - T = \overline{pCO_2} * \exp(0.0423 * (SST - \overline{SST}))$$
$$pCO_2 - nonT = pCO_2 * \exp(0.0423 * (\overline{SST} - SST))$$

Through experimental processes Takahashi verified that the effects of temperature and dissolved carbon concentrations dominate the levels of pCO_2 in the surface ocean (Takahashi et al. 1993). The first equation above shows a positive relationship between $pCO_2^{s.ocean}$ and temperature meaning an increase in SST causes an increase in $pCO_2^{s.ocean}$. Likewise, a directly proportional relationship exists between $pCO_2^{s.ocean}$ and salinity but is insignificant when compared to the impact of temperature.

Included in the pCO_2-nonT equation above are the remaining non-temperature components DIC and ALK as well as the negligible effect of SSS. These two dominant chemical properties have opposing effects on $pCO_2^{s.ocean}$. As DIC increases, the overall amount of carbon in the system increases, subsequently increasing $pCO_2^{s.ocean}$ levels. Conversely, ALK is inversely proportional to DIC (Sarmiento and Gruber 2006) and therefore an increase in ALK would act to lower surface ocean pCO_2 values. DIC and ALK are impacted by advection, convection, freshwater flux, and biological activity further

complicating the pCO_2-nonT component.

In addition, the physical circulation patterns of the global ocean can further complicate the surface ocean dynamics. For example, colder waters, while typically having lower pCO_2 levels, also are denser subsequently driving increased mixing which brings waters high in DIC to the surface due to an accumulation of DIC at depth caused by the "biological pump". Therefore these two effects (pCO_2-T and pCO_2-nonT) can often act in opposition to one another (Gruber et al. 2002; Takahashi et al. 2002; McKinley et al. 2006).

4. RESULTS

i. Decadal Results: 1981-1995

Trends calculated for years spanning 1981 thru 1995 represent uptake tendencies of the various biomes on a relatively short timescale, which should include influences from climactic variations including the North Atlantic Oscillation (NAO) and the El Niño-Southern Oscillation (ENSO). We term this 15-year timescale "decadal" because it is consistent with the shot-term variability in major climate indices such as ENSO or NAO. Model versus sampled model analyses suggest that a 15-year timescale is the lower limit of capturing a trend due to limited data coverage in early years resulting in large errorbars (Figures 13-15).

A global area-weighted trend for this subset of years is 1.2885 ± 0.4928. For comparison, the area-weighted average trend in $pCO_2^{s.ocean}$ only considering the 16 biomes confirmed by the models is 1.2401 ± 0.4789. Both of these global trends are indistinguishable from the atmosphere (1.45 ± 0.07 µatm/yr), reflecting a constant ΔpCO_2 over time, and thus a steady global ocean sink for 1981-1995.

$pCO_2^{s.ocean}$ trends

At the decadal timescale, 14 of the 16 biome's $pCO_2^{s.ocean}$ trends are indistinguishable from the atmospheric trend (1.45 ± 0.07 µatm/yr). In the North Pacific, the SUB and SES biome $pCO_2^{s.ocean}$ trends are indistinguishable from the atmosphere (errorbars cross the atmospheric trend line). Only the North Pacific permanently stratified subtropical (PSS) and Pacific equatorial (EQU) biomes result in trends below the atmospheric level, thus representing an increasing sink

in those regions. In the South Pacific, North Atlantic, South Atlantic, Indian Ocean, Southern Ocean, and LLU biomes, the $pCO_2^{s.ocean}$ trend is consistent with the atmospheric rate of increase. Therefore, in a majority of the world ocean, during a decadal timescale of 1981-1995 the observations show an ocean sink that is remaining constant with respect to atmospheric trends. However, large errorbars on the trends, resulting from sparse data, may make it difficult to distinguish any real trends on this timescale.

pCO_2-nonT and pCO_2 –T trends

On decadal timescales, nearly half of the global biomes are dominated solely by the pCO_2-nonT component of $pCO_2^{s.ocean}$, while three others are influenced by both pCO_2-nonT and pCO_2 –T, but with pCO_2-nonT having the dominant impact. Five biomes are influenced primarily by pCO_2 –T, while one biome has insufficient coverage to determine which is the driving force (Figure 10 a-d). Despite these differences, no biome reports a pCO_2-nonT trends significantly less than zero.

In the North Pacific, the SUB biome is dominated by the temperature component of pCO_2 with calculations reporting a declining temperature trend. In the North Pacific SES and PSS biomes pCO_2-nonT acts as the dominant driver with temperature trends indistinguishable from zero. The Pacific EQU biome is dominated by a positive trend in the pCO_2-T component while the South Pacific PSS is dominated by the pCO_2-nonT component. In the South Pacific SES biome

both components contribute to the $pCO_2^{s.ocean}$ trend with observations reflecting a decline in the temperature and a strong increase in the pCO_2-nonT.

In the North Atlantic SUB biome both components have an impact on the $pCO_2^{s.ocean}$ trend, with temperature showing a strong decline over the 15-year time span and pCO_2-nonT showing a strong increase. Further south, the North Atlantic SES and PSS biomes are primarily driven by pCO_2-nonT with temperature trends indistinguishable from zero. Alternatively, the Atlantic EQU biome is dominated solely by a positive temperature trend. In the South Atlantic PSS biome, $pCO_2^{s.ocean}$ trends are also driven by positive trends in the temperature component, while in the South Atlantic SES biome we are unable to tell which component is dominating as they both are indistinguishable from zero.

The Southern Ocean SUB biome is dominated by increasing temperatures, leaving the pCO_2-T trend as the dominant factor in $pCO_2^{s.ocean}$ increase in this region.

Indian PSS trends are driven by pCO_2-nonT while the neighboring SES biome in the Indian Ocean is dominated by both the pCO_2-nonT and pCO_2-T components. Global LLU regions also exhibit a small rate of increase in pCO_2-nonT.

ii. Multi-Decadal Results

When trends are calculated over a 30-year period spanning 1981 thru 2010, many more biomes have trends in $pCO_2^{s.ocean}$ significantly different from the in pCO_2^{atm} (1.66 ± 0.07 µatm/yr). This difference, as compared to the

decadal timescale, can partially be attributed to more observations resulting in smaller confidence intervals during this longer time series. However, by looking at this longer time span, I am also able to smooth out the effects of climatic oscillations and better distinguish the long-term mean trend and its driving mechanisms.

The global area-weighted trend, including all biomes, is 1.4979 ± 0.1954 while the average trend when only including biomes that are confirmed by the model is slightly larger: 1.5323 ± 0.1915. Regardless of this choice, the global-average surface ocean pCO_2 trend is indistinguishable from the atmosphere (1.66 ± 0.07 μatm/yr).

pCO_2 trends

Trend analyses for three decades of observations result in five biomes with trends significantly lower than the 30-year atmospheric pCO_2 trend, one biome higher than the atmosphere and 10 biomes indistinguishable from the atmospheric trend (Figure 11).

Results for the Pacific Ocean are shown on the left of Figure 11. In the North Pacific, the SUB biome $pCO_2^{s.ocean}$ trend is significantly less than the atmospheric trend, indicating an increasing carbon sink in that region while the North Pacific SES and PSS biome trends are indistinguishable from the atmospheric trend. Moving toward the south, the Pacific EQU and South Pacific PSS biomes also both have $pCO_2^{s.ocean}$ trends below the atmospheric rate,

indicating increasing sinks in those regions. The South Pacific SES is increasing at a steady rate as compared to the atmosphere.

In the North Atlantic, the SUB, SES, and PSS biomes all display trends in $pCO_2^{s.ocean}$ that are indistinguishable from the atmospheric increase in carbon dioxide, while the Atlantic EQU biome reports an increasing sink due to a $pCO_2^{s.ocean}$ trend distinguishable and less than that of the atmosphere. The South Atlantic PSS biome trend has a steady carbon sink as the calculated trend is consistent with that of the atmosphere while the South Atlantic SES biome has a $pCO_2^{s.ocean}$ trend significantly less than the atmosphere, thus suggesting an increasing carbon sink in this region.

The Southern Ocean trend is indistinguishable from the atmospheric trend over this longer timescale.

Only the Indian PSS biome is significantly greater than the atmospheric trend while the Indian SES biome is increasing at a trend consistent with pCO_2^{atm}. Global LLU regions also exhibit a constant carbon sink.

pCO_2-nonT and pCO_2 –T trends

On a multi-decadal timescale, the impact of temperature (pCO_2-T) on the overall $pCO_2^{s.ocean}$ trend decreases as compared to the pCO_2-T impact on decadal timescales. On decadal timescales, the chemistry (pCO_2-nonT) component emerges as the dominant factor controlling $pCO_2^{s.ocean}$ in a majority of the world's oceans (Figure 12 a-d). Regardless of differences in temperature trends over the biomes, all of the global biomes have pCO_2-nonT trends

significantly greater than zero, suggesting an increase in anthropogenic carbon concentrations in the global oceans, as found by independent methods in previous studies (Sabine et al. 2004, Khatiwala et al. 2009).

As shown in Figure 12a, the North Pacific SUB biome's increasing sink is due to a declining temperature trend counteracted by increasing pCO_2-nonT. Increases in both pCO_2-nonT and pCO_2-T are evident in the North Pacific SES biome, however not at sufficient magnitudes to produce a $pCO_2^{s.ocean}$ trend that differs from the atmospheric trend. The constant sink in the North Pacific PSS biome also is due to the pCO_2-nonT component. The Pacific EQU biome is dominated by pCO_2-nonT, and there is also a slight increase in temperature, but still, this region is an increasing sink. In the South Pacific PSS, the increasing sink is dominated by the pCO_2-nonT component. The South Pacific SES biome is influenced by a small decline in temperature however the temperature change is unable to counteract the large increase in pCO_2-nonT that ultimately dominates the $pCO_2^{s.ocean}$ trend.

As shown in Figure 12b, a steady sink in the North Atlantic SUB biome is influenced by a decline in temperatures, and compensated by a large increase in the pCO_2-nonT component. The North Atlantic SES and PSS biomes are primarily driven by pCO_2-nonT, with temperature trends indistinguishable from zero. Likewise, the Atlantic EQU biome is dominated by a positive non-temperature trend, but of a smaller magnitude, such that the total pCO_2 trend is less than the atmosphere. The South Atlantic SES and PSS biomes both exhibit increasing trends in temperature over the 30 years as well as increases in pCO_2-

nonT components. Given the magnitudes in each region, the PSS biome remains a constant sink with respect to pCO_2^{atm} while SES is an increasing sink.

Increasing trends in both temperature and pCO2-nonT drives the Southern Ocean SUB biome, however the pCO_2-T trend remains the dominant factor influencing carbon uptake over this region (Figure 12c).

As shown in Figure 12d, the SES biome in the Indian Ocean also exhibits high pCO_2-nonT trends but temperature trends in the region are not different from zero. The decreasing sink of the Indian PSS biome is dominated by strong increases in pCO_2-nonT in combination with an increase in pCO_2-T, which collectively produce a trend in $pCO_2^{s.ocean}$ greater than in pCO_2^{atm}. The global LLU region also exhibits a significant rate of increase in pCO_2-nonT and temperature changes near zero.

iii. Sensitivity of Results to End Year Chosen

With many biomes reporting significant differences in trends and driving mechanisms between the two timeseries analyzed here it leads to the question, what is the sensitivity of these trends to the years selected? In Figures 13-15, I show trends calculated, beginning in 1981 and ending in each year between 1990 and 2010. In these figures, the black line represents the $pCO_2^{s.ocean}$ trend as it fluctuates depending on the end year chosen for the calculation (1990-2010). The gray shading symbolizes the confidence interval on the $pCO_2^{s.ocean}$ trend. The dashed line and pink shading represents the atmospheric pCO_2 trend

(with corresponding uncertainties) while the blue and green lines correspond to the trend of temperature and pCO_2-nonT components of the $pCO_2^{s.ocean}$ trend respectively. Years where the trend lines are blanked-out are years where no data is available and therefore the trend is the same as for the previous year that does contain data.

From these plots it is clear that the $pCO_2^{s.ocean}$ trends and its dominant component can fluctuate depending on end year chosen for analysis. Also, while errorbars are very large for trends with end years in the 1990s, they become significantly smaller as more data is included in the analysis.

In the Pacific Ocean, both middle and high latitude (SUB and SES biomes) pCO_2-T trends are significantly different from zero and exhibit large fluctuations over short and intermediate length timescales (until roughly end year 2000). These fluctuations decrease and pCO_2-T trends approach zero (however sometimes still remain significantly higher or lower) when considering timescales exceeding 20 years. In the PSS biomes of the Pacific Ocean, the time it takes for temperature fluctuations to converge near zero is much shorter, occurring after only 15 years. In both Pacific PSS biomes (NP-PSS and SP-PSS) the pCO_2-T trends do converge to zero while the pCO_2-nonT trends are clearly dominant and track the $pCO_2^{s.ocean}$ trend. In the Pacific EQU biome the dominant mechanism fluctuates between pCO_2-T and pCO_2-nonT for end years in the 1990s, undoubtedly due to ENSO variability. However, when considering a 20+ year timeframe, pCO_2-nonT emerges as the dominant driver while pCO_2-T approaches zero.

In the Atlantic Ocean, the high latitude SUB region again reflects pCO_2-T trends significantly different from zero on the short and intermediate length timeseries and does not approach zero until over 25 years of data are considered. pCO_2-nonT, however, is important to the overall $pCO_2^{s.ocean}$ trend on both short and long timescales. North Atlantic SES and PSS and the South Atlantic SES biomes require a much shorter time for the pCO_2-T trend to approach zero (15-20 years). In each of these biomes the pCO_2-nonT trend clearly tracks the $pCO_2^{s.ocean}$ trend beginning around 1995, showing its dominance as the controlling mechanism of change. The Atlantic Ocean EQU biome has limited temporal data coverage resulting in large errorbars on calculated trends, making this type of analysis difficult. In the South Pacific PSS biome the pCO_2-T trend dominates over all years however leveling off of both pCO_2-nonT and pCO_2-T trends occurs for longer timeseries lengths (final year 2001-2010) and the effect of pCO_2-nonT is equivalent to that of pCO_2-T.

The Southern Ocean SUB biome (Figure 15) demonstrates a compensating effect between the pCO_2-nonT and pCO_2-T trends in maintaining a consistent $pCO_2^{s.ocean}$ trend. The pCO_2-nonT dominates the trend only for analysis ending in 2000-2004, after which time the pCO_2-T emerges again as the dominant mechanism. However, with their corresponding errorbars, both components of pCO_2 are indistinguishable from one another and both are significantly above zero.

In the Indian Ocean SES biome the data is sporadic in annual coverage. Trends in pCO_2-nonT are always important to the trend in $pCO_2^{s.ocean}$. The trend

in pCO_2-T approaches zero only in 2008. In the PSS biome, in timeseries shorter than 15 years, the effects of temperature are critical. Timescales longer than 15 years are dominated by carbon accumulation, accelerating the $pCO_2^{s.ocean}$ trend in 1998 and leveling off around the atmospheric rate by year 2000. In LLU regions of the global ocean pCO_2-nonT consistently dominates the surface ocean trend on timescales longer than 10 years (final year 1991-2010). On all timescales temperature trends do not significantly differ from zero.

5. DISCUSSION

i. Global

On a global scale, this analysis of multi-decadal surface ocean pCO_2 trends reveals that the ocean carbon sink is increasing at a rate consistent with that of the atmosphere. Le Quéré et al. (2010) find the global ocean to be a net source of pre-industrial carbon based on model analysis spanning years 1981-2007 while their regional observational analysis reveals areas of both a net carbon source and sink. Le Quéré et al. hypothesizes that the ocean pCO_2 trends should be increasing at a rate that lags behind the atmosphere in carbon uptake due to both its slow mixing rate between the surface and the deep ocean as well as air-sea gas transfer processes (Le Quéré et al. 2010). Their findings, based on model analysis, suggest that the total effect of climate change and variability on air-sea flux trends has been to weaken the global oceanic CO_2 sink. This conclusion does not agree with our analysis of global observations.

While temperature fluctuations contribute to uptake trends on a decadal timescale, the magnitude of temperature's impact decreases on the whole when considering changes on multi-decadal timescales. The short-term, large-scale cooling that we see from $pCO_2^{s.ocean}$ trends calculated between 1981-1995 could be linked to the eruption of Mt Pinatubo in 1991 which released aerosols into the atmosphere that effectively reduce the amount of incoming solar radiation that reaches the surface oceans.

In a majority of the world's oceans, the non-temperature component of $pCO_2^{s.ocean}$ trends dominates on both decadal and multi-decadal timescales. This signal of trends being dominated by chemistry is consistent with the buildup of anthropogenic carbon in the world's oceans (Sabine et al. 2004; Khatiwala et al. 2009).

By considering how the $pCO_2^{s.ocean}$ trend changes in response to the end date chosen for analysis (Figures 13-15) we can compare the impacts of temperature and chemistry components over 30 years included in this analysis. While large fluctuations in both trends are observed on shorter timescales, we see a clear dominance of pCO_2-nonT trends as analysis is extended to span 15 to 20 years. This emergence occurs earlier in more tropical biomes (Pacific PSS, Atlantic SES and PSS) whereas it takes roughly 20 years for pCO_2-nonT to become dominant in subpolar biomes (Pacific and Atlantic SUB). Temperature trends converge to near zero in a majority of the biomes after 15-20 years, suggesting that they may be linked to climatic variability such as the NAO and ENSO and will therefore be averaged out when considering longer timescales.

Additionally, the pCO_2-T and pCO_2-nonT components work together to allow $pCO_2^{s.ocean}$ to approximately follow the atmospheric trend. To accomplish this, the two components compensate for one another and keep the $pCO_2^{s.ocean}$ trend relatively steady (Figures 13-15). For example, a warming trend in pCO_2-T results in less of an increase in pCO_2-nonT because warming decreases carbon uptake due to solubility effects. This is evident in the SO-SUB, NP-SES, PAC-EQU, and SA-SES and SA-PSS biomes. Alternatively, a cooling trend in pCO_2-T

results in an increasing trend in pCO_2-nonT, as is the case in the NP-SUB, SP-SES, and NA-SUB biomes. Because cooling results in more carbon uptake and lower $pCO_2^{s.ocean}$ values, the pCO_2-nonT would need to increase to keep the overall trend in $pCO_2^{s.ocean}$ steady.

ii. North Pacific

SUBPOLAR

Due to limited available data, pCO_2 trends on decadal timescales (1981-1995, Figure 9) in the SUB biome of the North Pacific (NP-SUB) have large error bars making them indistinguishable from the atmospheric trend. However, when including all 30 years of data (1981-2010) signals of an increasing carbon sink emerge due to a pCO_2 trend below that of the atmosphere (Figure 11). These trends agree with previous studies by Takahashi et al. (2006) and Le Quéré et al. (2009) who found rates of change in $pCO_2^{s.ocean}$ to be similar to or slower than the atmospheric rate in much of the subpolar North Pacific.

Both the temperature component and the non-temperature component act as driving mechanisms for this sink. The temperature trend in the region shows a slight decline over the decades, thus acting to lower pCO_2 values. This decrease in temperature is consistent with observations of temperature inversions in regions of the subarctic North Pacific, which would cause cooler waters to be measured in the surface layer of the ocean (Ueno et al. 2005). While these inversions vary spatially in the region, a majority of available pCO_2

observations lies in the northern Gulf of Alaska, an area that commonly exhibits temperature inversions.

The trend in the non-temperature component is not clearly distinguished. Given the large uncertainty, accumulation of CO_2 in the surface ocean may have occurred on the decadal timescale, and has occurred to some degree over the 30 years, but it is difficult to say how rapidly. If there was, in fact, a slower increase in carbon here, it may be that there is a replenishing supply of waters with comparatively low anthropogenic DIC from depth as a result of the tidal mixing against the bathymetry of the area. Bringing waters low in anthropogenic DIC to the surface will allow continued uptake from the atmosphere by depleting the positive pCO_2-nonT trend. The significantly declining temperatures have suppressed $pCO_2^{s.ocean}$ and promoted an increasing sink in this region.

SEASONALLY STRATIFIED SUBTROPICAL

During both the decadal and multi-decadal timescale, the NP-SES biome in the North Pacific shows a trend consistent with the atmosphere (Figure 9, 11). On the longer timescale there is a slight warming trend in the temperature observations (Figure 12a). Cool SSTs emerged in the early 1980s around the latitude of the Kuroshio–Oyashio Current, east of Japan, and these cold anomalies persisted through the end of the decade. This region of cooling is associated with a southward displacement of the latitude at which the subpolar and subtropical gyres converge (Seager et al. 2001). Therefore, the warming

trend emerging from our analysis could be biased by the dates selected for analysis (beginning during the decade of noticeable cooling).

The dominant mechanism in this region is pCO_2-nonT with strong increases on both the short and long timescales analyzed (Figures 10a and 12a). By looking at a timeseries of the trend, calculated beginning in 1981, but with a varying end year (Figure 13b) we see that although there have been fluctuations in the magnitude and direction of both the pCO_2-nonT and pCO_2 –T components, the pCO_2-nonT has remained the driving mechanism since 1990. Another interesting observation is that the pCO_2-nonT and pCO_2 –T trends seem to fluctuate in opposition, in a way compensating for a change in one another. A decrease in the pCO_2 –T trend in the late 1990s (which would act to lower the $pCO_2^{s.ocean}$) is compensated by an increase in the pCO_2-nonT trend, thus holding the $pCO_2^{s.ocean}$ trend relatively constant.

PERMANENTLY STRATIFIED SUBTROPICAL

On a decadal timescale the NP-PSS biome reports an increasing carbon sink (Figure 9) however when the analysis is extended out to 2010 the trend changes to reflect carbon uptake at a rate consistent with the atmosphere (Figure 11). In both cases the trend is dominated by pCO_2-nonT (Figure 10a, 12a).

These results are consistent with Takahashi et al. (2006) who found the $pCO_2^{s.ocean}$ in much of the subtropical gyre to be increasing at decadal rates indistinguishable from the atmosphere. However, these results differ from other studies (Keeling et al. 2004; Dore et al. 2003) that found the $pCO_2^{s.ocean}$ to be

increasing faster than pCO_2^{atm}, although these studies analyze a different subset of years. Keeling et al. (2004) founds, at station ALOHA near Hawaii, a strong increase in $pCO_2^{s.ocean}$ trends around 1997, which he attributes to a decrease in precipitation. By looking at the trends calculated with varying end years (Figure 13c) we can see how the $pCO_2^{s.ocean}$ trend has fluctuated over the years, previously reflecting an increasing sink in the region (trends below 1 μatm/yr during the early 1990s) but increasing in the past 15 years to reflect a steady carbon sink. The dominant driver of this increasing trend is clearly shown to be the pCO_2-nonT component as it increases at a similar rate over the last 15 years. Figure 13c also clearly shows that the pCO_2-nonT component did not emerge as the driving mechanism until nearly 2000, thus reflecting the dominance of the buildup of carbon on the $pCO_2^{s.ocean}$ trend over the previous two decades.

These fluctuations in the driving mechanism support the idea that the $pCO_2^{s.ocean}$ trend is driven by changes in chemistry, which is consistent with the buildup of anthropogenic carbon in the world oceans. The NP-PSS biome encompasses much of the subtropical gyre, which is an area of downwelling. The increase in pCO_2-nonT is not likely due to DIC rich waters being brought up from depth but is instead likely due to an increase in carbon entering the ocean at the surface, thus balancing the increasing pCO_2^{atm}.

EQUATORIAL

In the equatorial Pacific biome, I find an increasing sink for both timescales, however the dominant mechanism changes from temperature at the

decadal timescale to the non-temperature component at the multi-decadal timescale (Figure 10a, 12a). As shown in Figure 13d, it takes a few decades before the pCO_2-nonT emerges as the dominant control of the $pCO_2^{s.ocean}$ trend while the magnitude of pCO_2-T decreases as you move to longer timescales. This pattern is consistent with a buildup of anthropogenic carbon over long timescales once climatic events (ENSO, PDO) are averaged out. Also of note is the high sensitivity in the trend calculated from 1981-1995 as compared to 1981-1996. With just one year of added data the trends shift so that the pCO_2-nonT component jumps to dominate the trend as the temperatures exhibit a slight decline. The $pCO_2^{s.ocean}$ trend increases sharply to be near the pCO_2^{atm} trend when the analysis includes years 1981 through 1996. This fluctuation could be related to the end of a strong El Niño period spanning 1991-1995 and the subsequent transition into a La Niña conditions during 1996 and 1997.

On the longer timescale, there is a positive trend in the temperature in the EQU biome. Observations in this biome are concentrated in the central Pacific region, which corresponds to the Nino 3.4 region used in ENSO-related studies. The dominance of strong El Niño events during the past three decades (1983, 1987, 1992, 1997, 2003) as compared to strong La Niñas could be contributing to this increasing temperature trend as El Niño events would cause a warm pool of water to extend across the equatorial Pacific due to a weakening of upwelling waters in the east (Trenberth 1997). This decrease in upwelling causes less cold, nutrient-rich deep water to be brought to the surface.

The trend in pCO_2-nonT is below the atmospheric trend, which drives the total $pCO_2^{s.ocean}$ trend. As in the NP SUB biome, the connection to the deep waters, which contain low anthropogenic DIC, may also damp the accumulation of anthropogenic CO_2 in the Pacific equatorial region.

Because data collected during ENSO events are included in this analysis we have also split this biome into an East and West section (divided at 170W) and analyzed their respective trends. The number of monthly data points between these two areas does not vary considerably (N=136 in the west, N=141 in the east during years 1981-2010). On the multi-decadal timescale, the eastern equatorial Pacific has a larger $pCO_2^{s.ocean}$ trend (1.47 ±0.3) than the western equatorial Pacific (1.09 ±0.2) although they are indistinguishable from one another when including 1σ confidence bounds for each. The western EQU biome trend does fall below that of the atmospheric trend, resulting in an increasing sink in this half of the biome.

Both eastern and western regions are dominated by the non-temperature component, however only the western half of the biome reports an increase in pCO_2-T (0.38 ±0.12) in addition to pCO_2-nonT (0.68 ±0.3). The trend in pCO_2-nonT is significantly greater in the eastern half of the region (1.43 ±0.5), thus resulting in a higher $pCO_2^{s.ocean}$ trend despite no significant change in the temperature in the eastern Pacific.

These trends are not consistent with findings by Le Quéré et al (2009) who reported a positive trend in ΔpCO2 ($pCO_2^{s.ocean}$ - pCO_2^{atm}), reflecting a declining sink in this region. While the areas analyzed are not identical, this

discrepancy is more likely due to differences in analysis methods and years selected than spatial areas analyzed as neither the east nor west regions of the Pacific EQU biome reported declining carbon sinks.

iii. South Pacific

PERMANENTLY STRATIFIED SUBTROPICAL

The subtropical gyre of the South Pacific (SP-PSS) yields a sink indistinguishable from the atmosphere on the short-term but an increasing sink on the multi-decadal timescale. This result is consistent with the findings of Le Quéré et al. (2009) through both their model and data analysis, although the results from their observational study were based on only a few 10°x10° boxes in the western subtropical gyre, as opposed to including data over the whole width of the basin as is done here. The increase in data included in our analysis primarily comes from a frequented ship track across the subtropical gyre of the South Pacific (Figure 2).

Changing chemistry in the region drives the SP-PSS $pCO_2^{s.ocean}$ trend. While temperature trends remain indistinguishable from zero, the pCO_2-nonT component far exceeds this level on both timescales considered in this analysis, confirming the theory of a buildup of anthropogenic carbon in the surface ocean of this region. While Takahashi et al. (2002) reported that the basin was primarily a source of carbon to the atmosphere, their fluxes varied between east and west with the western half of the subtropical gyre having a flux much closer to zero.

Because available data is concentrated in the western half of the basin (Figure 2) it is reasonable that our calculations concluded an increasing sink.

SEASONALLY STRATIFIED SUBTROPICAL

In the SES biome of the South Pacific (SP-SES) both decadal and multi-decadal timescales reflect an increase in $pCO_2^{s.ocean}$ indistinguishable from that of the atmosphere (Figure 9, 11). Both are dominated by increasing pCO_2-nonT trends, and also reflect slight cooling trends over the respective timescales (Figure 10a, 12a). This opposition between driving mechanisms is consistent with Currie et al. (1998) who found that the biological effect (i.e. a removal of carbon with cooler temperatures) was greater in magnitude and opposite in direction to the temperature trends, specifically in the area of convergence just east of New Zealand. With the large errorbars on the respective trend calculations for this biome, this is clearly a region of the global ocean where more observations would allow significant improvements to be made in carbon flux and uptake trend analysis.

iv. North Atlantic

SUBPOLAR

In the SUB biome of the North Atlantic (NA-SUB), both decadal and multi-decadal timescales reflect an increase in $pCO_2^{s.ocean}$ indistinguishable from that of the atmosphere. Both are dominated by increasing pCO_2-nonT trends, but also reflect cooling trends over both timescales (figure 10b, 12b). This dominant

mechanism is consistent with a buildup of anthropogenic carbon in the region's surface ocean.

Cooling trends in subpolar North Atlantic waters are not commonly found in other analyses (Thomas et al. 2008; Ullman et al. 2009). Thomas et al. (2008) shows that temperature trends can vary in magnitude and direction depending on years selected for analysis. While on shorter timescales (1991-1996, 1997-2004) Thomas et al. (2008) find a warming trend over the subpolar region of the North Pacific, when considering a longer timescale (1979-2004) a cooling trend emerges.

The reasoning for a decrease in SST trends as found in our analysis could be the specific location of the available measurements (Figure 2). The SUB biome covers a large area including the area dominated by the North Atlantic Drift Current (NADC), a slow-moving body of water between Iceland and Ireland. The temperature of the surface waters of the NADC almost always exceeds that of both surrounding waters and the overlying atmosphere (Rossby 1996). A large fraction of data collected in this biome comes from this area (Figure 2) and therefore this anomalous warm pool could result in negative trends if earlier measurements were centralized in this area while later observations were from regions outside of this anomalous regime. However, given that this biome covers much of the subpolar gyre (an area of divergence and upwelling of cooler waters), a seasonal bias in data collection may also contribute to the declining temperature trends. Clearly there is a need for more data collection in this biome.

Previous studies by Lefevre et al. (2004) and Corbiere et al. (2007) yielded declining sinks in the subpolar North Atlantic. Major differences in the database used for analysis (SURATLANT data only versus Takahashi database) and years analyzed could explain this disagreement.

SEASONALLY STRATIFIED SUBTROPICAL

In the NA-SES biome the trend in surface ocean pCO_2 is entirely due to pCO_2-nonT with temperature fluctuations indistinguishable from zero on either timescale (Figure 10b, 12b). The results for $pCO_2^{s.ocean}$ trends consistent with the atmosphere are not in agreement with those found by Schuster & Watson (2007) and Schuster et al. (2009) who found $pCO_2^{s.ocean}$ trends higher than the atmosphere. This is likely due to a difference in analysis methods. Schuster et al. (2009) calculated trends and corresponding confidence intervals using binned observations (resulting in a larger N value) as opposed to values averaged over grid cells as is done in this study (See Methodology section for further discussion).

Changes in subpolar circulation and convective mixing in response to climate variability is consistent with decadal trends of $pCO_2^{s.ocean}$ in this region (Thomas et al. 2008; Ullman et al. 2009). Further understanding of the links between physical variability in this region and the NAO and Atlantic Multidecadal Oscillation, as well as the potential impacts on the carbon cycle, are needed. However, our results support an accumulation of anthropogenic DIC in the ocean at a rate equal to the accumulation rate in the atmosphere.

PERMANENTLY STRATIFIED SUBTROPICAL

Likewise, in the NA-PSS biome, the trend in surface ocean pCO_2 is indistinguishable from the atmosphere and is entirely due to an increase in pCO_2-nonT with temperature fluctuations indistinguishable from zero for both timescales (Figure 10b, 12b). The results of the carbon sink in this biome are consistent with analyses by Bates et al. (2007) and Gruber et al. (2002) who focused their analysis on a single long-term data timeseries near Bermuda (Bermuda Atlantic Ocean Time Series (BATS)). Our results support a steady $pCO_2^{s.ocean}$ trend in this region increasing in a manner consistent with the accumulation of anthropogenic DIC.

EQUATORIAL

On decadal timescales, the Atlantic EQU (ATL-EQU) biome displays a carbon sink consistent with that of the atmosphere driven primarily by an increase in temperature (Figure 10b). Typically equatorial upwelling zones are areas of substantial CO_2 uptake because of the constant resupply of older thermocline waters (low in anthropogenic carbon) to the surface. The decadal trends calculated here could be heavily influenced by climatic events such as the NAO and therefore are inconsistent with this tendency.

When considering the multi-decadal analysis, reporting an increasing sink in the region dominated by pCO_2-nonT and temperature trends near zero, the expected system reemerges (Figure 12b). The transition to dominance by the pCO_2-nonT mechanism could be due to enhanced upwelling during the long

timescale, bringing up low-anthropogenic carbon waters, which allow for an increasing carbon sink. Evident both in Figure 2 and 14d, data in this region is very sparse, resulting in large uncertainty. This area shows strong evidence of a region requiring more data collection.

v. South Atlantic

PERMANENTLY STRATIFIED SUBTROPICAL

On both the decadal and multi-decadal timeframe the South Atlantic PSS (SA-PSS) biome's constant carbon sink is dominated by an increase in temperature (Figure 10b, 12b). This warming trend is consistent with that found in the equatorial Atlantic. The PSS biome, encompassing much of the subtropical gyre, is an area of convergence and thus downwelling. Further research would help in the understanding of the warming trend revealed in this analysis as it may have to do with a southward strengthening of the southern hemisphere subtropical gyres due to a changing wind stress curl over the Southern Ocean.

Separate from the temperature trend shown, the strength of the pCO_2-nonT component strengthens between decadal and multi-decadal analysis in this biome. These results are consistent with a buildup of anthropogenic carbon in the region over multiple decades.

SEASONALLY STRATIFIED SUBTROPICAL

The poleward section of the subtropical gyre in the South Pacific is encompassed by the SES biome (SA-SES). While on decadal timeseries the SES biome emerges as a consistent sink with neither mechanism statistically different from zero, a multi-decadal analysis reveals a different scenario. When analyzing over three decades the SA-SES biome reflects an increasing carbon sink with a trend significantly less than the pCO_2^{atm} trend (Figure 11). Positive trends in both pCO_2-nonT and pCO_2-T emerge as significant mechanisms with nearly equal contributions from each (Figure 12b). Similar to the NP-SES biome, this SA-SES biome's overall $pCO_2^{s.ocean}$ trend decreases with respect to pCO_2^{atm} while both temperature and pCO_2-nonT are greater than zero. Limited data in this region could be a concern and contribute to inconclusive evidence available to explain these trends.

vi. Southern Ocean

SUBPOLAR

Similar to the PSS biome in the South Atlantic, the Southern Ocean SUB (SO-SUB) biome's $pCO_2^{s.ocean}$ trend is increasing at a rate consistent with the atmosphere. Likewise, the trend is dominated by an increase in temperature while an increase in pCO_2-nonT also contributes (Figure 12c). The warming temperatures of the Southern Ocean waters have been observed by other research groups including Gille (2002). While measured warming trends have been made at intermediate depths, the overturning circulation patterns of the

Southern Ocean suggest that this signal should, on long timescales, spread throughout the water column, resulting in trends consistent with our observational analysis.

While the temperature trend does not change significantly between the two timescales analyzed, the contribution of pCO_2-nonT does increase when considering longer timeseries (Figure 10c, 12c). A strong connection to the deep ocean is characteristic of the Southern Ocean due to its circulation patterns, windy conditions, and cold temperatures. Therefore, pCO_2-nonT trends may be damped by this characteristic mixing that would act to replenish the region with waters from depth that would be lower in anthropogenic carbon.

Previous studies have found the Southern Ocean carbon sink to be weakening relative to the expected sink from rising atmospheric carbon concentrations (Le Quéré et al. 2007; Lovenduski et al. 2008). Differences between our methodology and these studies include the use of model output rather than observational data as well as differing subsets of years for each analysis. However, Lovenduski et al. reasons for a declining sink include a buildup of anthropogenic carbon, which cannot rule out based on the conclusions stated here. However we see a damping of this effect, possibly due to the high degree of connectivity between deep and surface waters in this region.

vii. Indian Ocean

PERMANENTLY STRATIFIED SUBTROPICAL

Despite an effort in the 1990s to increase the carbon database observations for the Indian Ocean (Metzl 2009), there are still relatively few direct measurements in the basin (Figure 2). Additionally, complex circulation patterns and seasonal monsoons contribute to the strong possibility of a seasonal bias in trend calculations. While our analysis for the IND-PSS biome shows a transition in the biome's carbon sink from a constant sink during the decadal timeseries to a declining sink during the multi-decadal timeseries, this could be strongly influenced by seasonal coverage. During the N-E monsoon the Indian Ocean contains relatively high pCO_2 values whereas strong coastal upwelling during the S-W monsoon disperses this water and reduced the carbon content overall (Sabine et al. 2000).

In addition to seasonal variations in pCO_2, the Indian Ocean carbon content varies latitudinally with northern hemisphere and equatorial regions having values above atmospheric levels (thus a net efflux) whereas the southern hemisphere portion of the basin typically has lower $pCO_2^{s.ocean}$ values. While our trend calculations differ from previous studies by Metzl et al. (1998), further analysis considering the seasonal and hemispheric coverage must be considered.

A warming trend was also observed over the multi-decadal timescale (Figure 12d), which is consistent with warming, specifically during austral winter,

identified by Metzl (2009). He concluded that a reduction of DIC in surface waters must counteract the uptake of anthropogenic carbon. This could be accomplished by enhanced biological productivity.

SEASONALLY STRATIFIED SUBTROPICAL

While the $pCO_2^{s.ocean}$ trend remains consistent with the atmosphere at both long and short timescales in the Indian Ocean's SES (IND-SES) biome, the driving mechanisms change. On a decadal timescale the trend is driven by both a decrease in the temperature of the region as well as an increase in the pCO_2-nonT component (Figure 10d). The temperature trend is possibly related to the high index state of the Southern Annular Mode (SAM) during the 1990s (Metzl 2009) which would tend to decrease winter temperatures in the region.

Trends on a multi-decadal timescale are instead dominated by the pCO_2-nonT component while temperature changes remain slightly above zero (Figure 12d). This dominant chemical component could be due to both an increase of DIC import in addition to amplified uptake of anthropogenic carbon. Increased westerlies around this latitudinal band of the southern hemisphere would cause deep mixing, bringing DIC-rich waters to the surface (Metzl 2009).

viii. Low Latitude Upwelling

Global regions of upwelling, typically along coastal waters, have cold water, and high carbon characteristics as a result of the upwelling circulation patterns around coastal margins. Trends in $pCO_2^{s.ocean}$ reflect a carbon sink

consistent with that of the atmosphere. While cooler temperatures are typical in these regions, a significant change in temperature is not dominating the trend in surface carbon concentration. Instead the $pCO_2^{s.ocean}$ trend for LLU regions is dominated by pCO_2-nonT, consistent with an accumulation of anthropogenic carbon in the surface oceans. Given that deep, low-anthropogenic-carbon waters are being upwelled, the increase in magnitude of the pCO_2-nonT trend between decadal and multi-decadal timescales supports a steady uptake of anthropogenic carbon at the surface in LLU regions.

6. CONCLUSIONS

i. Conclusions

The main goal of this thesis was to utilize both observations and model output to develop a methodology to calculate global ocean carbon uptake trends. The magnitude of carbon uptake by the global oceans will depend on how the ocean responds to increases in ocean warming and stratification, which can drive both increases in CO_2 uptake through biological and export changes, and decreases through solubility and density changes. Overall, pCO_2 variability is constrained by opposing effects due to SST and DIC. By analyzing $pCO_2^{s.ocean}$ trends and decomposing them into temperature and non-temperature components we were able to determine the driving mechanisms of ocean uptake trends over the past three decades. This analysis of surface ocean pCO_2 observations reports an increase in global ocean carbon levels consistent with that of the atmosphere.

On decadal timescales a majority of the regions analyzed report $pCO_2^{s.ocean}$ trends indistinguishable from the trend in atmospheric pCO_2. Both temperature and chemical mechanisms drive these changes. Cooling trends are observed in 4 of the 16 biomes including both the North Pacific and North Atlantic SUB biomes as well as the Indian and South Pacific SES biomes. Warming was seen in four other biomes: the Southern Ocean SUB, South Atlantic PSS, and both Pacific and Atlantic Equatorial regions. Non-temperature trends are consistently above zero in a majority of the biomes.

At the multi-decadal timescale, a greater number of biomes have trends significantly different from the atmospheric trend, though the global area-weighted average for the thirty-year analysis resulted in trends indistinguishable from the atmosphere. Driving mechanisms varied from region to region, however, in all of the biomes the non-temperature component was statistically greater than zero, a trend consistent with the buildup of anthropogenic carbon in the surface oceans.

The non-temperature component acts as the dominant mechanism in a majority of the biomes, however this only occurs on longer timescales (Figures 13-15). For tropical regions including the PSS biomes this dominance emerges after roughly 15 years whereas it takes nearly a decade longer in more polar regions of the ocean (SUB biomes).

While temperature trends have varied between decadal and multi-decadal timescales (Figure 10, 12) in many of the global biomes, the temperature component exhibits a warming trends overall between the two timescales

considered with only 4 biomes showing statistical cooling on the multi-decadal timescale. Despite this overarching warming of global biomes, the $pCO_2^{s.ocean}$ trend remains consistent with the atmospheric pCO_2 trend. The forcing responsible for this is the compensating effect of the pCO_2-nonT component on $pCO_2^{s.ocean}$ trends. As warming of the ocean continues, this study suggests that the trend in $pCO_2^{s.ocean}$ will continue to approximately follow the trend in pCO_2^{atm}. A negative feedback on the ocean carbon sink is expected (Le Quéré et al. 2010), but this analysis suggests we do not have sufficient data to show this yet.

ii. Future work

Detection of feedbacks between carbon-climate systems is of great interest to both scientists and policy-makers, however clear signals are often masked by decadal-timescale variability. If anthropogenically-forced climate change is directly modulating the natural components of the global carbon cycle it will take decades of observational data to provide sufficient evidence. Comparison of various studies can be difficult and often results in fuel for competing interests.

Calculations of carbon flux between the ocean and atmosphere will help to provide comparisons between this analysis and other ocean carbon studies. Flux calculations depend on wind-stress relationships to calculate gas exchange between the atmosphere and ocean. Such relationships are still highly debated in the ocean carbon community (Nightingale et al. 2000; Wanninkhof 1992; Liss 1974). Improvement of such techniques will improve flux calculations.

Additionally, verifying SST trends resulting from this analysis utilizing global

SST datasets such as Had1SST (Rayner et al. 2003) and Reynolds SST Analysis (Reynolds et al. 2002) will provide further confirmation of sufficient data coverage in both time and space. Improved and expanded $pCO_2^{s.ocean}$ datasets, such as the SOCAT database due to be released later this year, will aid in improving trends and analysis of ocean sinks by shrinking confidence intervals.

REFERNCES

Antonov, J.I., et al. (2006), W*orld Ocean Atlas 2005, Volume 2: Salinity* S. Levitus, Ed., NOAA Atlas NESDIS 62, U.S. Government Printing Office, Washington, D.C., 182 pp.

Bates, N. R. (2007). Interannual variability of the oceanic CO_2 sink on the subtropical gyre of the North Atlantic Ocean over the last 2 decades. *J. Geophysical Res.,* 112. C09013.

Bennington, V. et al (2009) What does chlorophyll variability tell us about export and air-sea CO2 flux variability in the North Atlantic, *Global Biogeochem. Cycles* 23, GB3002.

Canadell, J. et al. (2007), Contributions to accelerating atmospheric CO_2 growth from economic activity, carbon intensity, and efficiency of natural sinks. *Proc. Natl. Acad. Sci.* 104,18866-18870.

Corbiere, A., et al. (2007), Interannual and decadal variability of the oceanic carbon sink in the North Atlantic subpolar gyre. *Tellus B* 59, 168-178.

Currie, K.I., K. A. Hunter (1998), Surface water carbon dioxide in the waters associated with the subtropical convergence east of New Zealand. *Deep Sea Research I*, 45:1765–1777.

Delworth, T., et al. (2006), GFDL's CM2 global coupled climate models. Part I: Formulation and simulation characteristics, *J. Climate,* 19, 643–674.

Dickson, A. G. (1990), Standard potential of the reaction: AgCl (s)+1⁄2 H_2 (g)=Ag (s)+HCl (aq), and the standard acidity constant of the ion HSO_4 in synthetic seawater from 273.15 to 318.15 K, *J. Chem. Thermodyn. 22*, 113–127721.

Doney, S. C., et al. (2004), Evaluating global ocean carbon models: the importance of realistic physics, *Global Biogeochem. Cy*., 18, GB3017.

Dore, J.E. et al. (2003), Climate-driven changes to the atmospheric CO_2 sink in the subtropical North Pacific Ocean. *Nature*, 424, 754-757.

Doney, S. C., et al. (2009b), Skill metrics for confronting global upper ocean ecosystem-biogeochemistry models against field and remote sensing data, *J. Marine Syst*., 76, 95–112.

Friedlingstein, P., and Coauthors, 2006: Climate–Carbon Cycle Feedback Analysis: Results from the C4MIP Model Intercomparison. *J. Climate*, 19, 3337–3353.

Follows, M., Ito, T., & Dutkiewicz, S. (2006), On the solution of the carbonate chemistry system in ocean biogeochemistry models. *Ocean Model.* 12*,* 290-301.

Gille, Sarah T., (2002), Warming of the Southern Ocean Since the 1950s *Science* Vol. 295 no. 5558 pp. 1275-1277.

Ginoux, P., et al. (2001), Sources and distributions of dust aerosols simulated with the GOCART model, *J. Geophys. Res*., 106, 20255–20273.

Gruber, N. et al. (2002), Interannual variability in the North Atlantic ocean carbon sink, *Science*, 298, 2374-2378.

Henson, S.A. et al. (2010), Detection of anthropogenic climate change in satellite records. *Biogeoscience*s, 7, 621–640.

Keeling, C.D. et al. (2004), Seasonal and long-term dynamics of the upper ocean carbon cycle at Station ALOHA near Hawaii*. Global Biogeochemical Cycles*, 18. GB4006.

Keeling, C.D. and T.P. Whorf (2005), Atmospheric CO_2 records from sites in the SIO air sampling network. In Trends: A Compendium of Data on Global Change. Carbon Dioxide Information Analysis Center, Oak Ridge National Laboratory, U.S. Department of Energy, Oak Ridge, Tenn., U.S.A

Khatiwala et al. (2009), Reconstruction of the history of anthropogenic CO_2 concentrations in the ocean. *Nature* vol. 462 (7271) pp. 346-34.

Lefèvre, N. et al. (2004), A decrease in the sink for atmospheric CO_2 in the North Atlantic. *Geophys. Res. Letters*. Vol. 31 L07306.

Le Quéré, C. *et al*. (2009),Trends in the sources and sinks of carbon dioxide. *Nature Geoscience* 2, 831-836.

Le Quéré, C. *et al*. (2010) Impact of climate change on the global oceanic sink of CO_2. *Global Biogeochem. Cycles. In press*

Liss, P. S., et al. (1974), Flux of gases across the air-sea interface, *Nature*, 247, 181-184.

Locarnini, R.A., et al. (2006), *World Ocean Atlas 2005, Volume 1: Temperature.*

S. Levitus, Ed., NOAA Atlas NESDIS 61, U.S. Government Printing Office, Washington, D.C., 182 pp.

Lovenduski, N. et al. (2008), Towards a mechanistic understanding of the decadal trends in the Southern Ocean carbon sink. *Global Biogeochemical Cycles* 22, BG3016.

McKinley, G. A., et al. (2006), North Pacific carbon cycle response to climate variability on seasonal to decadal timescales, *J. Geophysical Research, 111,* C07S06.

Mehrbach, C., C. H. Culberson, J. E. Hawley, and R. M. Pytkowicz (1973), Measurement of the apparent dissociation constants of carbonic acid in seawater at atmospheric pressure, *Limnology and Oceanography, 18,* 897-907.

Metzl, N., et al., (1998), Seasonal and interannual variations of sea surface carbon dioxide in the subtropical Indian Ocean. *Mar. Chem.* 60, pp. 131–146.

Metzl, N. (2009) Decadal increase of oceanic carbon dioxide in Southern Indian Ocean surface waters (1991–2007). *Deep Sea Research II*, Vol 56, Issue 8-10. Pp 607-619.

Nightingale, P. D., et al. (2000a), Measurements of air-sea gas transfer during open ocean algal bloom. *Geophys. Res. Letters,* 27, 2117-2120.

Rayner N.A., et al. (2003), Global analyses of sea surface temperature, sea ice, and night marine air temperature since the late nineteenth century. *J Geophys Res.* 108:4407–4443.

Reynolds, R.W. and T.M. Smith (1994), Improved global sea surface temperature analyses using optimum interpolation. *J. Climate*, 7, 929-948.

Reynolds, R. W., et al. (2002). An improved in situ and satellite SST analysis for climate. *J. Climate*, 15, 1609-1625.

Reynolds R.W., et al. (2007), Daily high-resolution-blended analyses for sea surface temperature, *J. Climate* 20*,* 5473-5496.

Rossby, T. (1996), The North Atlantic Current and Surrounding Waters: At the Crossroads, *Review of Geophysics*, 34, 463-481.

Sabine, C.L., et al. (2000), Seasonal CO_2 fluxes in the tropical and subtropical Indian Ocean. *Marine Chemistry* 72, pp. 33–55.

Sabine, C.L. et al. (2004), The oceanic sink for anthropogenic CO_2, *Science*, 305(5682), 367-371.

Sarmiento, J.L., and N. Gruber (2002), Sinks for anthropogenic carbon, *Physics Today*, 30-36.

Sarmiento, J. L., et al. (2004), Response of ocean ecosystems to climate warming, *Global Biogeochem. Cycles*, 18.

Sarmiento, J. L. and N. Gruber (2006), Ocean Biogeochemical Dynamics. Princeton University Press, 503, pp.754.

Schuster, U., A. J. Watson (2007). A variable and decreasing sink for atmospheric CO_2 in the North Atlantic. *J. Geophysical Research, 112,* C11006.

Schuster, U. et al. (2009), Trends in North Atlantic seasurface fCO_2 from 1990-2006 *Deep Sea Research II* 56, 620-629.

Seager, R., et al. (2001), Wind-Driven Shifts in the Latitude of the Kuroshio–Oyashio Extension and Generation of SST Anomalies on Decadal Timescales *J. Climate*, 14, 4249–4265.

Takahashi, T., et al. (1993), Seasonal variation of CO_2 and nutrients in the high-latitude surface oceans: A comparative study, *Global Biogeochem. Cycles*, 7(4), 843–878.

Takahashi, T. *et al*. (2002), Global sea-air CO_2 flux based on climatological surface ocean pCO_2, and seasonal biological and temperature effects, *Deep-Sea Res. II* 49, 1601-1622.

Takahashi, T. *et al.* (2009), Climatological mean and decadal change in surface ocean pCO_2, and net sea–air CO_2 flux over the global oceans. *Deep-Sea Res. II* 56, 554- 577.

Takahashi, T., Sutherland, S.C. & Kozyr, *A. (2010), Global Ocean Surface Water Partial Pressure of CO_2 Database: Measurements Performed during 1957-2009 (Version 2009).* (ORNL/CDIAC-152, NDP-088r. CDIAC, ORNL, US DOE, Oak Ridge, Tennessee).

Tans, P. NOAA/ESRL (www.esrl.noaa.gov/gmd/ccgg/trends).

Thomas, H. et al. (2008), Changes in the North Atlantic Oscillation influence CO_2 uptake in the North Atlantic over the past 2 decades. *Global Biogeochem.*

Cycles 22, GB4027.

Trenberth, K. E., (1997), The Definition of El Niño. *BAMS*, 78, 2771-2777.

Ueno, H., I. Yasuda, (2005), Temperature Inversions in the Subarctic North Pacific. *J. Phys. Oceanogr.* 35, 2444–2456.

Ullman, D.J., McKinley, G.A., Bennington, V. & Dutkiewicz S. (2009), Trends in the North Atlantic carbon sink: 1992–2006. *Global Biogeochem. Cycles* 23, GB4011.

von Storch, H., F.W. Zwiers (2002), Statistical Analysis in Climate Research, 484 pp., Cambridge Univ. Press, Cambridge, U.K.

Wanninkhof , R. (1992), Relationship between wind speed and gas exchange over the ocean, *J. Geophys. Res*., 97, 7373–7382.

FIGURES

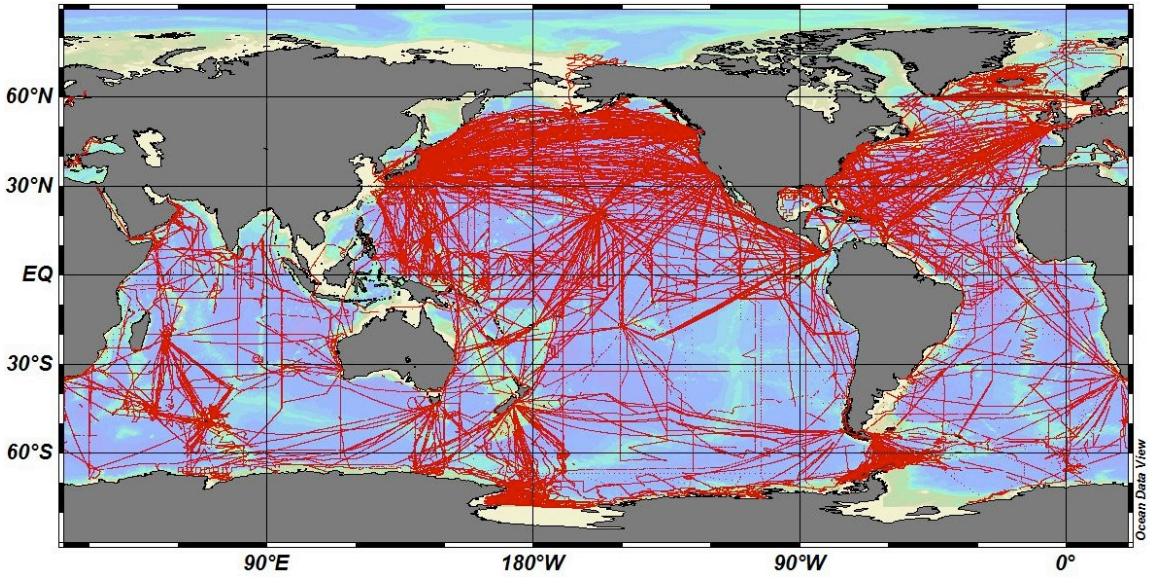

Figure 1. Ship tracks included in Takahashi's surface ocean pCO_2 database

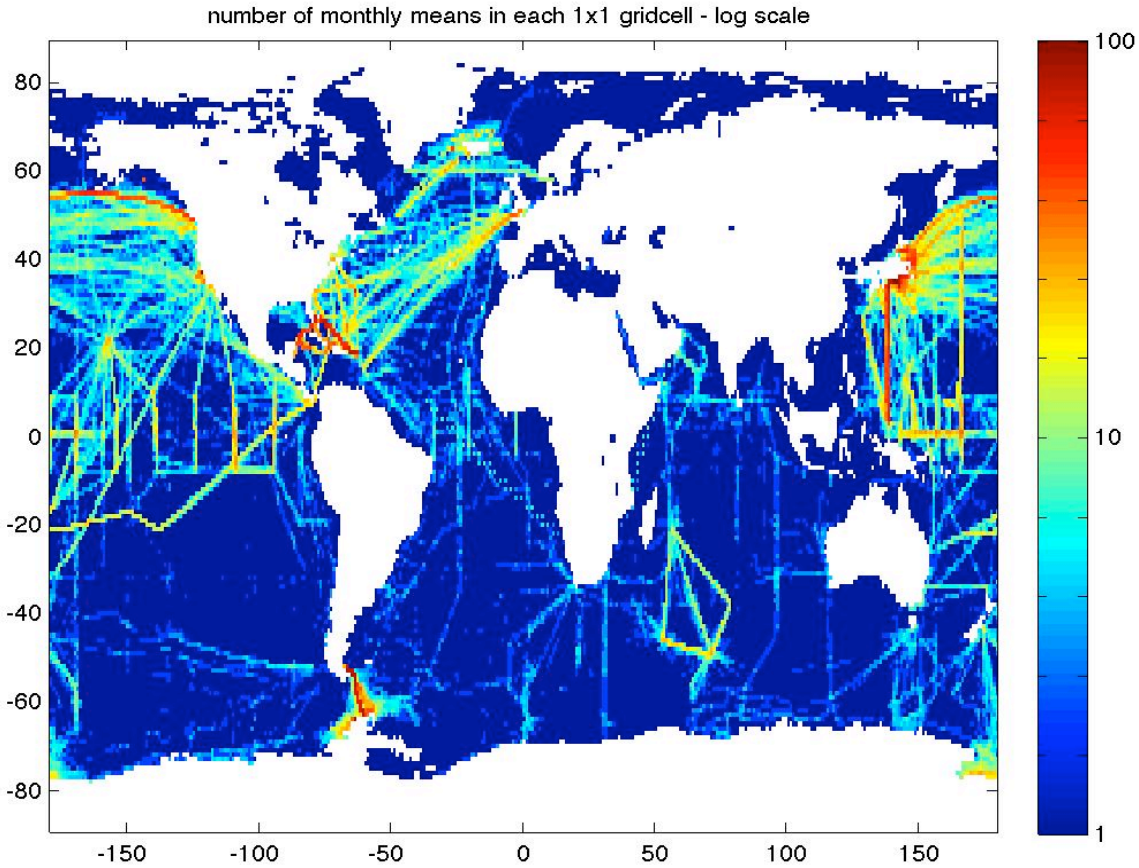

Figure 2. Spatial coverage of observations: number of monthly means in each 1° x 1° gridcell (log scale)

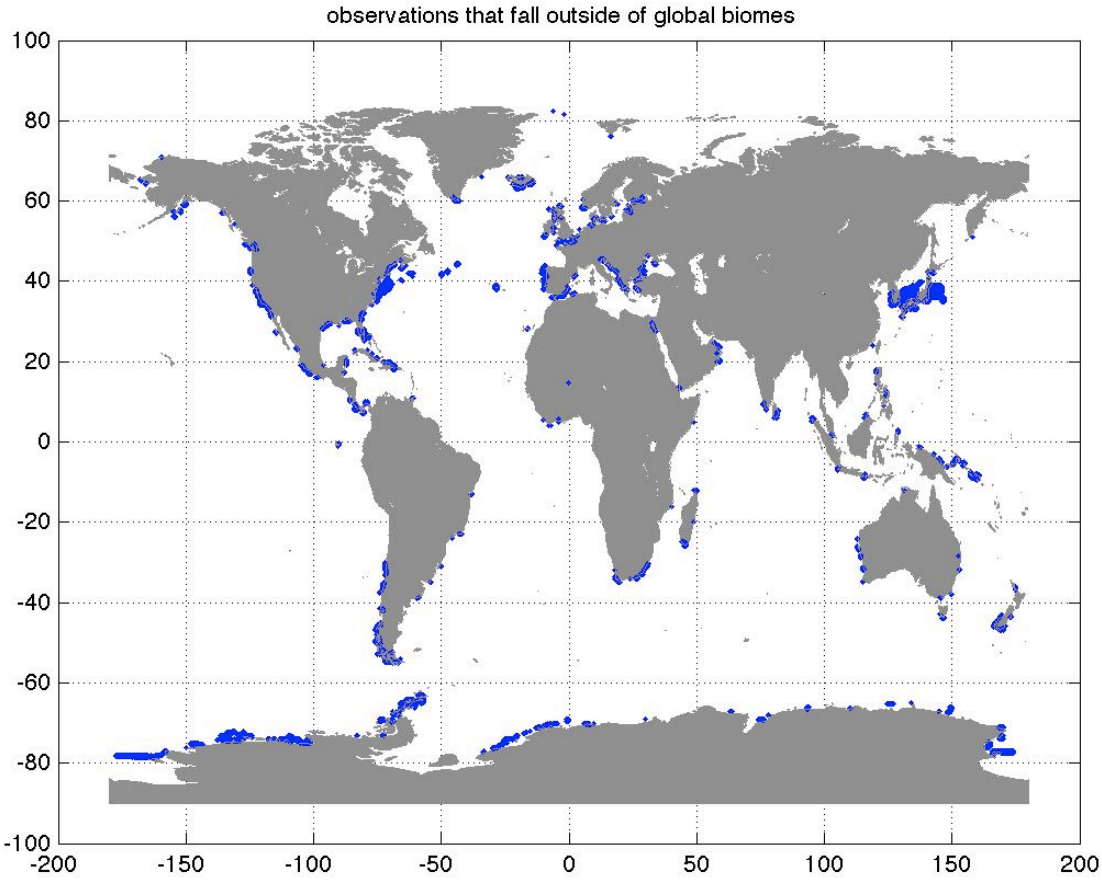

Figure 3. Observations that fall outside of the global biomes

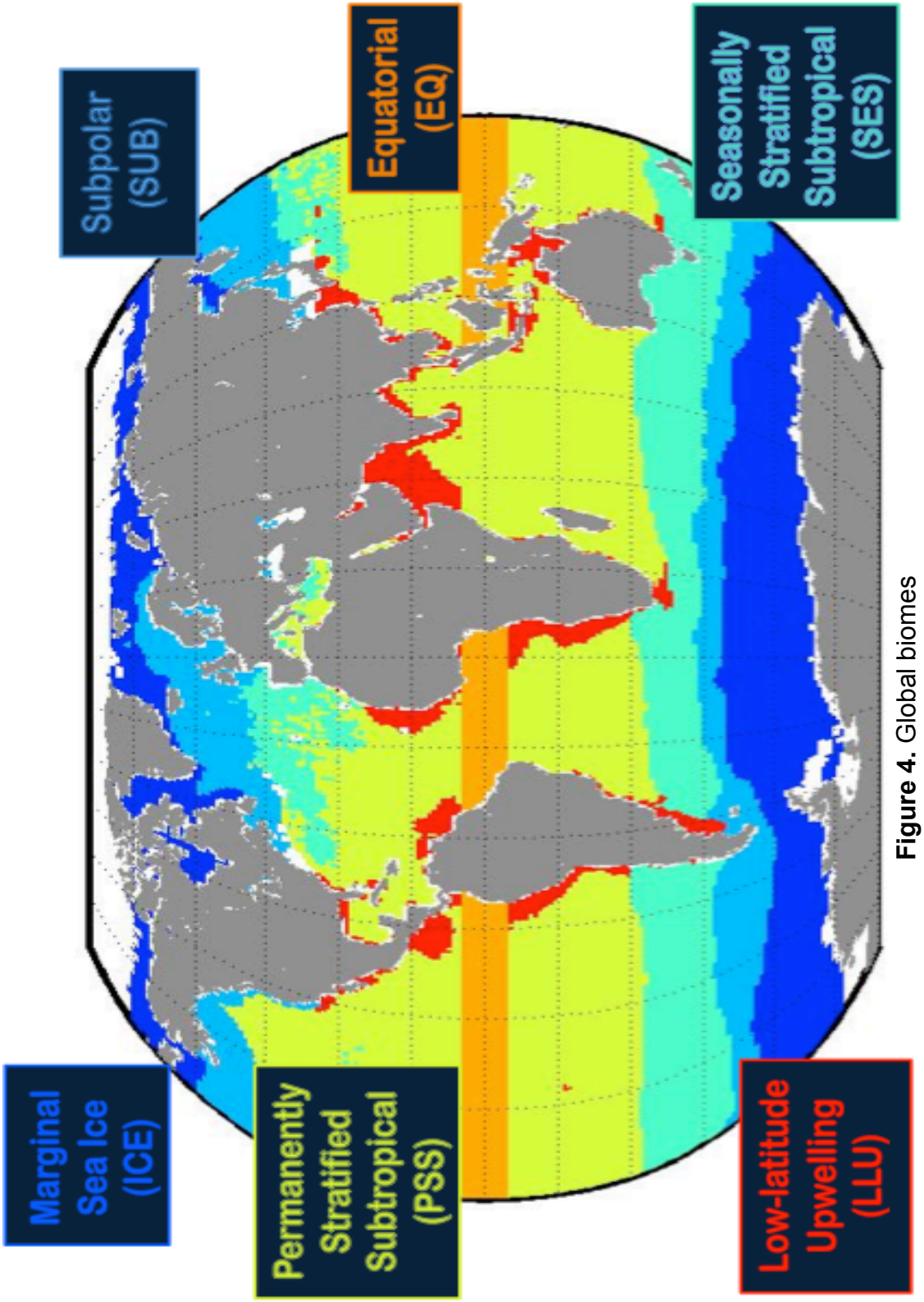

Figure 4. Global biomes

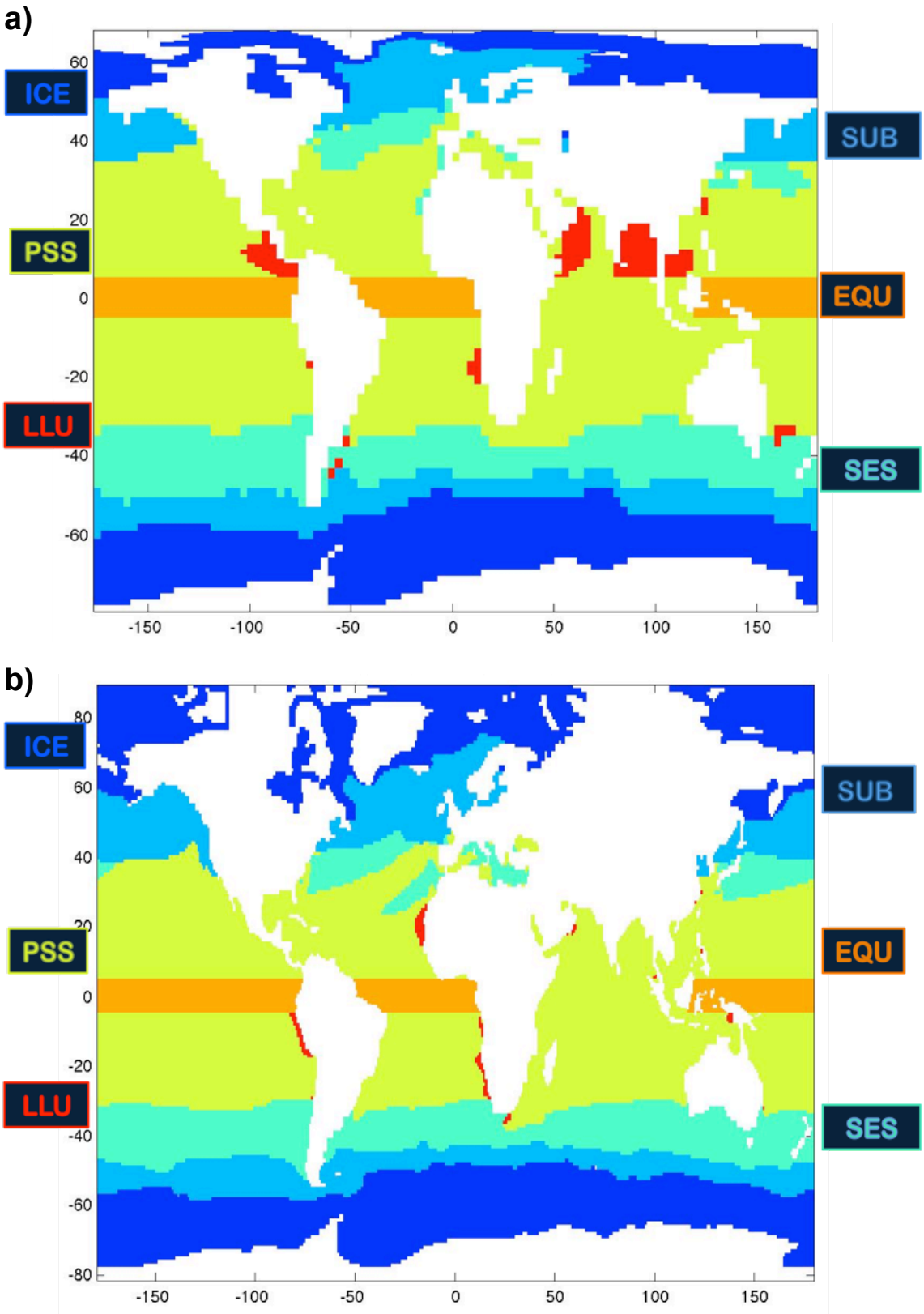

Figure 5. Global biomes for CCSM model (a) and MOM-TOPAZ model (b)

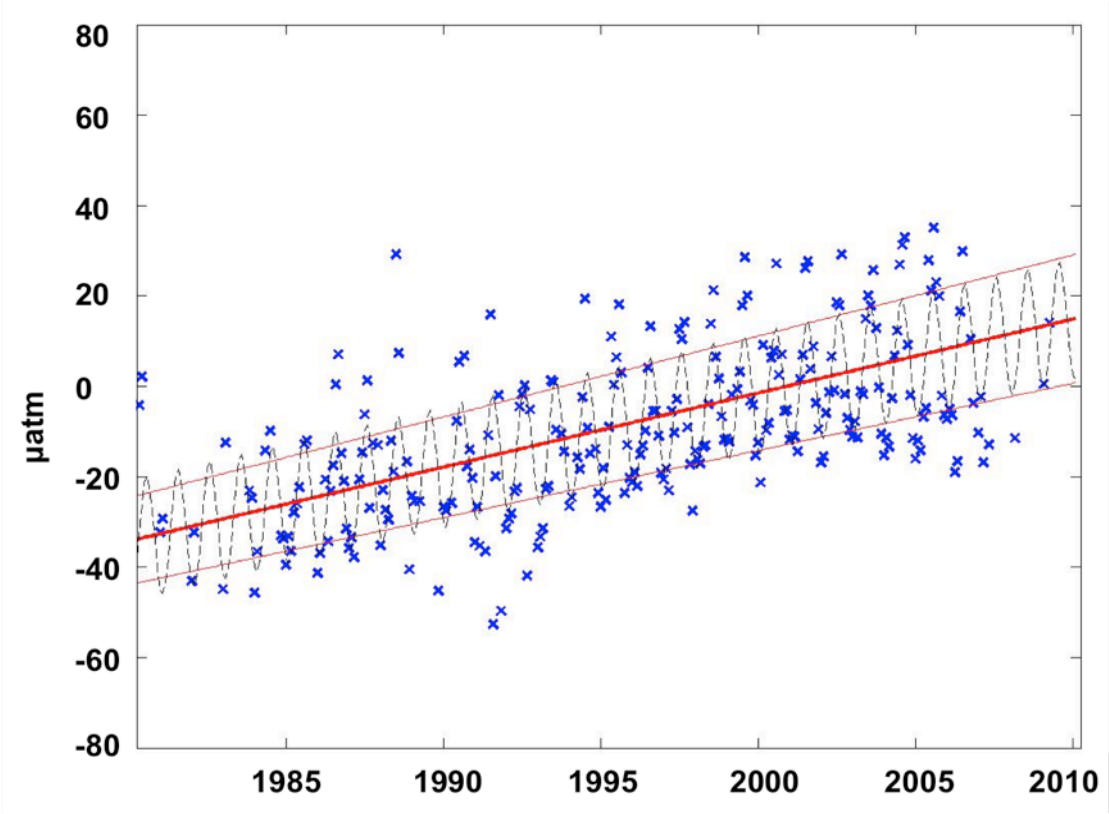

Figure 6. Timeseries of monthly mean anomalies (blue x) for North Pacific PSS biome. The assigned harmonic curve is shown by the dotted line, the linear trend by the bold red line, and corresponding 1σ confidence interval for linear fit by the thin red lines

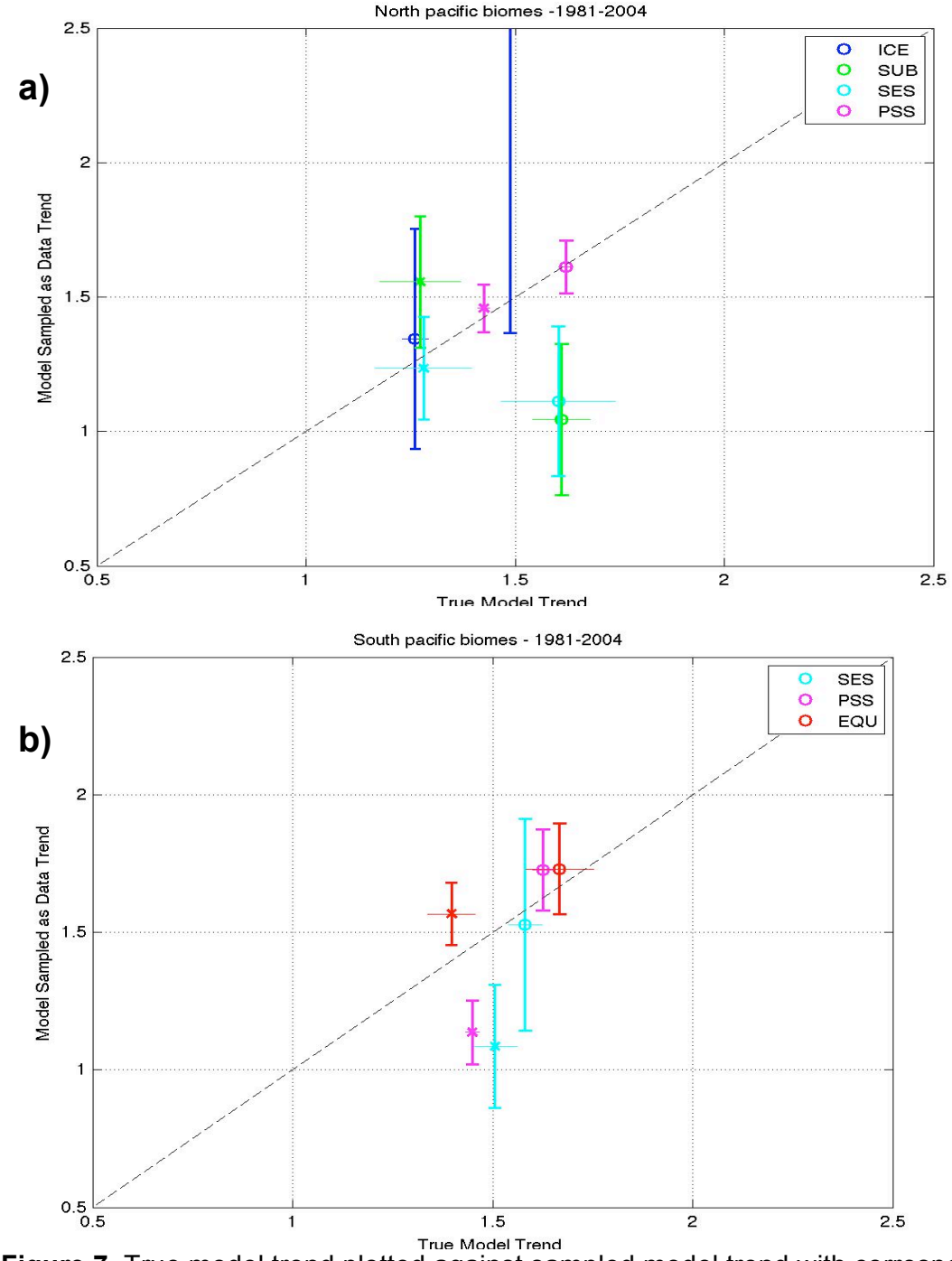

Figure 7. True model trend plotted against sampled model trend with corresponding 1σ CIs for each: N. Pacific (a), S. Pacific (b), N. Atlantic (c), S. Atlantic (d), Southern Ocean (e), and Indian Ocean (f). 'x' represents trends calculated using the MOM-TOPAZ model, 'o' represents trends from the CCSM model. Vertical and horizontal bars represent the confidence intervals for the sampled model and true model trends respectively. For biomes with CIs that cross the 1-to-1 (dashed) line, the biome is considered "confirmed" by the respective model.

c)

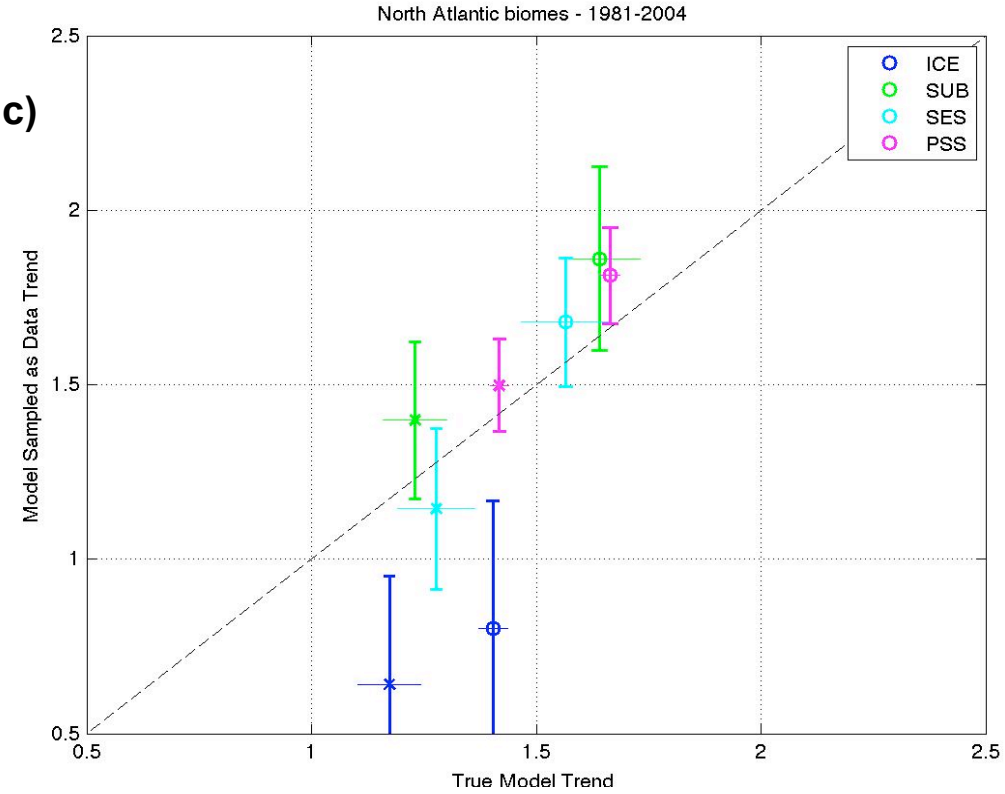
North Atlantic biomes - 1981-2004
ICE
SUB
SES
PSS
Model Sampled as Data Trend
True Model Trend
0.5
1
1.5
2
2.5

d)

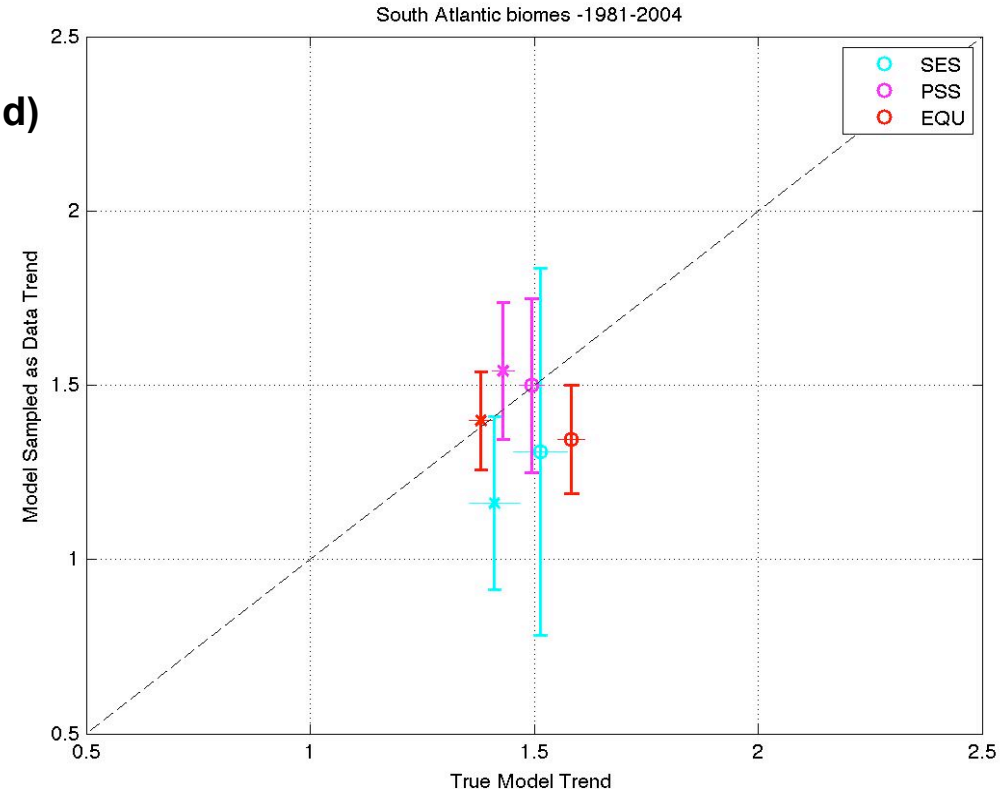
South Atlantic biomes -1981-2004
SES
PSS
EQU
Model Sampled as Data Trend
True Model Trend
0.5
1
1.5
2
2.5

e)

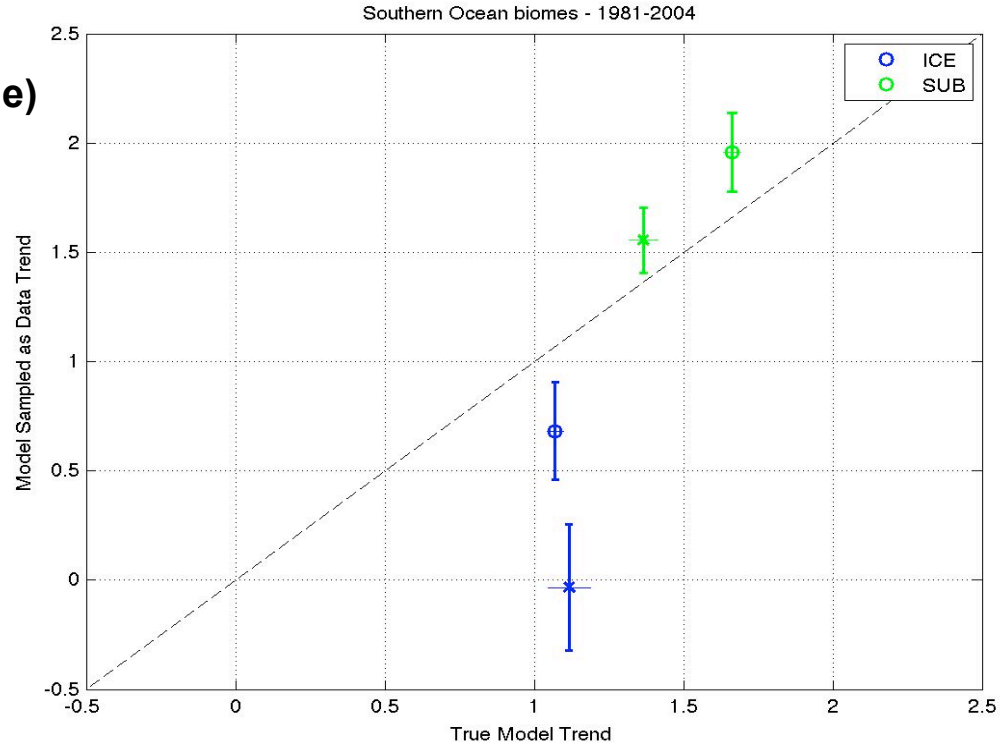
Southern Ocean biomes - 1981-2004
ICE
SUB
Model Sampled as Data Trend
True Model Trend
2.5
2
1.5
1
0.5
0
-0.5
-0.5
0
0.5
1
1.5
2
2.5

f)

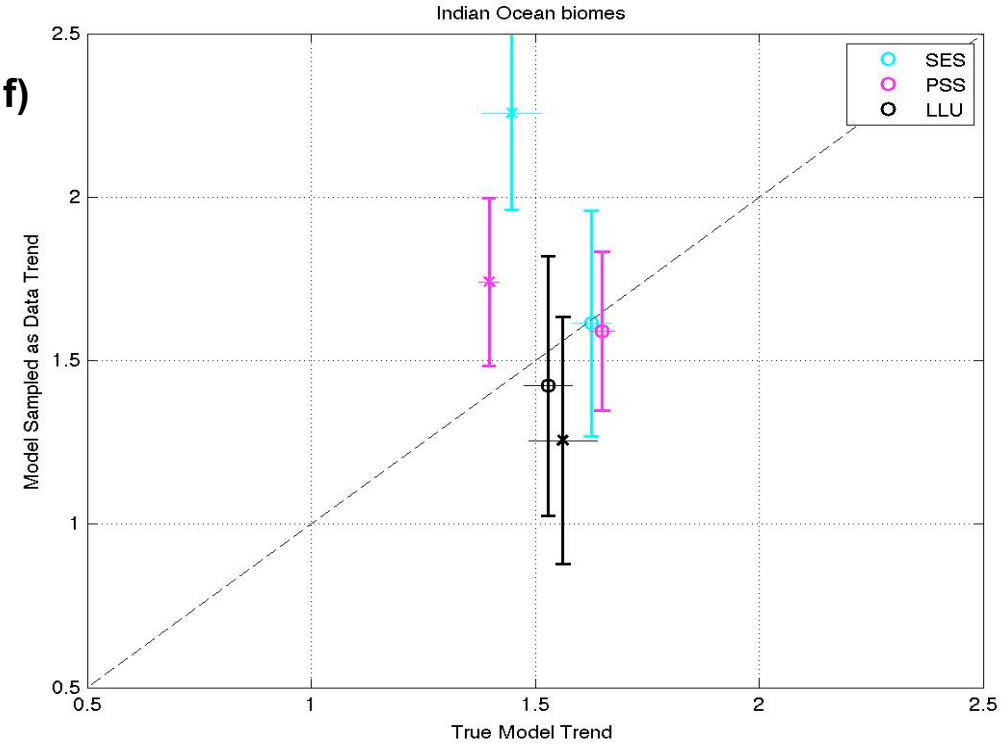
Indian Ocean biomes
SES
PSS
LLU
Model Sampled as Data Trend
True Model Trend
2.5
2
1.5
1
0.5
0.5
1
1.5
2
2.5

	1981 thru 1995		1981 thru 2004	
Biome	MOM-TOPAZ	CCSM3	MOM-TOPAZ	CCSM3
N Pacific ICE			X	X
N Pacific SUB		X	X	
N Pacific SES	X	X	X	
N Pacific PSS	X	X	X	X
Pacific EQU		X	X	X
S Pacific PSS	X	X		X
S Pacific SES	X	X		X
S Ocean ICE				
S Ocean SUB		X	X	
N Atlantic ICE	X	X		
N Atlantic SUB	X	X	X	X
N Atlantic SES	X	X	X	X
N Atlantic PSS			X	X
Atlantic EQU	X	X	X	
S Atlantic PSS	X	X	X	X
S Atlantic SES	X	X	X	X
Indian SES	X	X		X
Indian PSS	X	X		X
Global LLU	X	X	X	X

Table 2. Model verification by biome for both decadal (1981-1995) and multi-decadal (1981-2004) timespans. Biomes confirmed by at least one model on the multi-decadal timescale will be considered for further analysis.

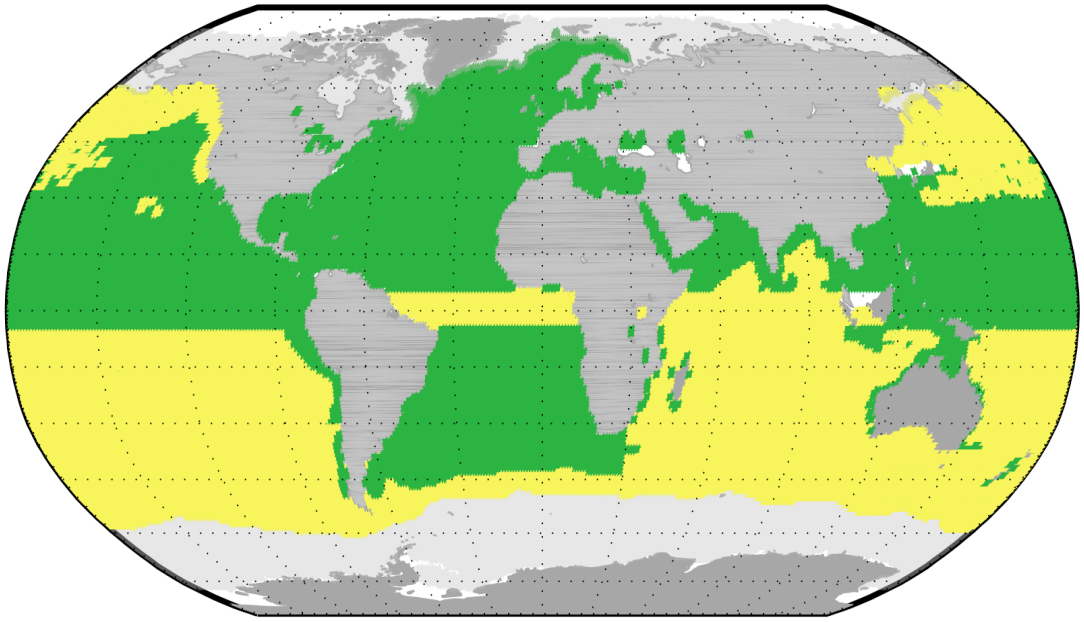

Figure 8. Map of confirmed biomes: Biomes confirmed by both models are in green, biomes confirmed by only one model are in yellow. Those confirmed by neither (NP-ICE, NA-ICE, SO-ICE) are in light gray.

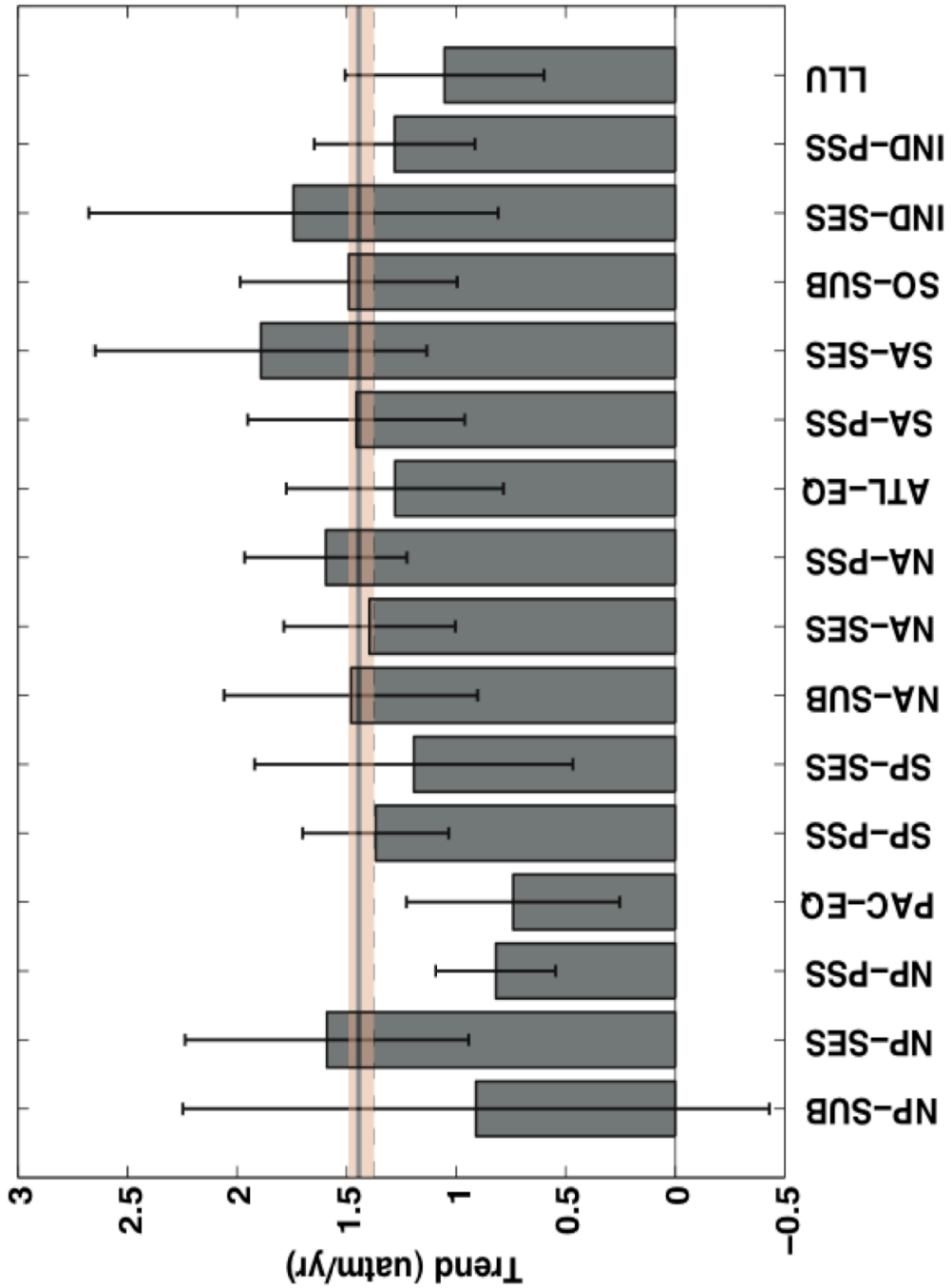

Figure 9. Bar plot showing trends in $pCO_2^{s.ocean}$ as compared to the atmospheric trend (represented by bold black line) for "decadal" timescale (years 1981-1995). 1σ confidence intervals for each biome's $pCO_2^{s.ocean}$ trend is represented by the vertical errorbars while the 1σ CI for the atmospheric trend is represented by the pink shaded region

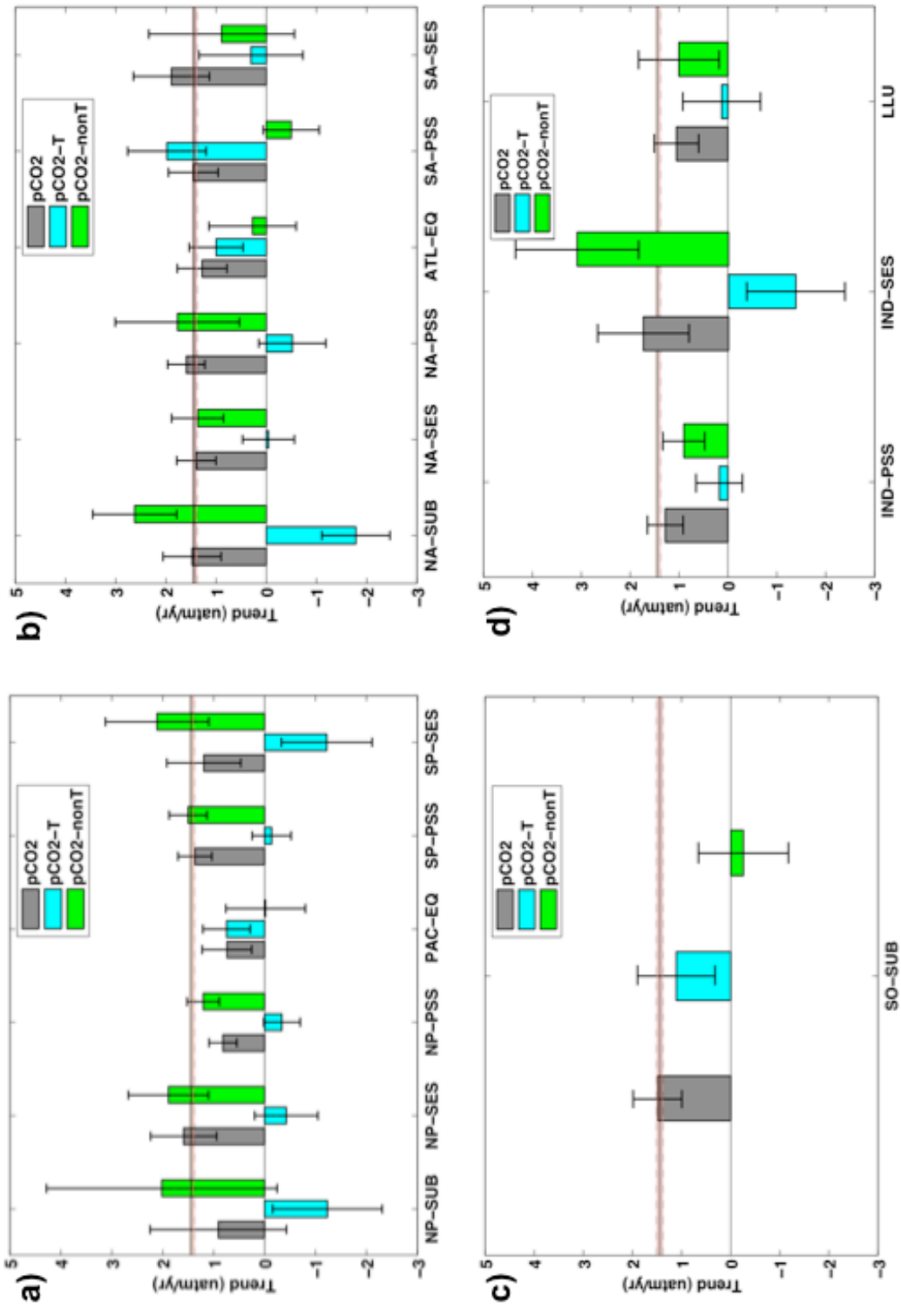

Figure 10. Decomposed pCO_2 trends for the decadal timescale (1981-1995), separated by ocean basin. Gray bars represent $pCO_2^{s.ocean}$ trends, blue bars represent pCO_2-T components and green bars represent pCO_2-nonT components. As in Figure 9, the atmospheric trend and errorbars are included.

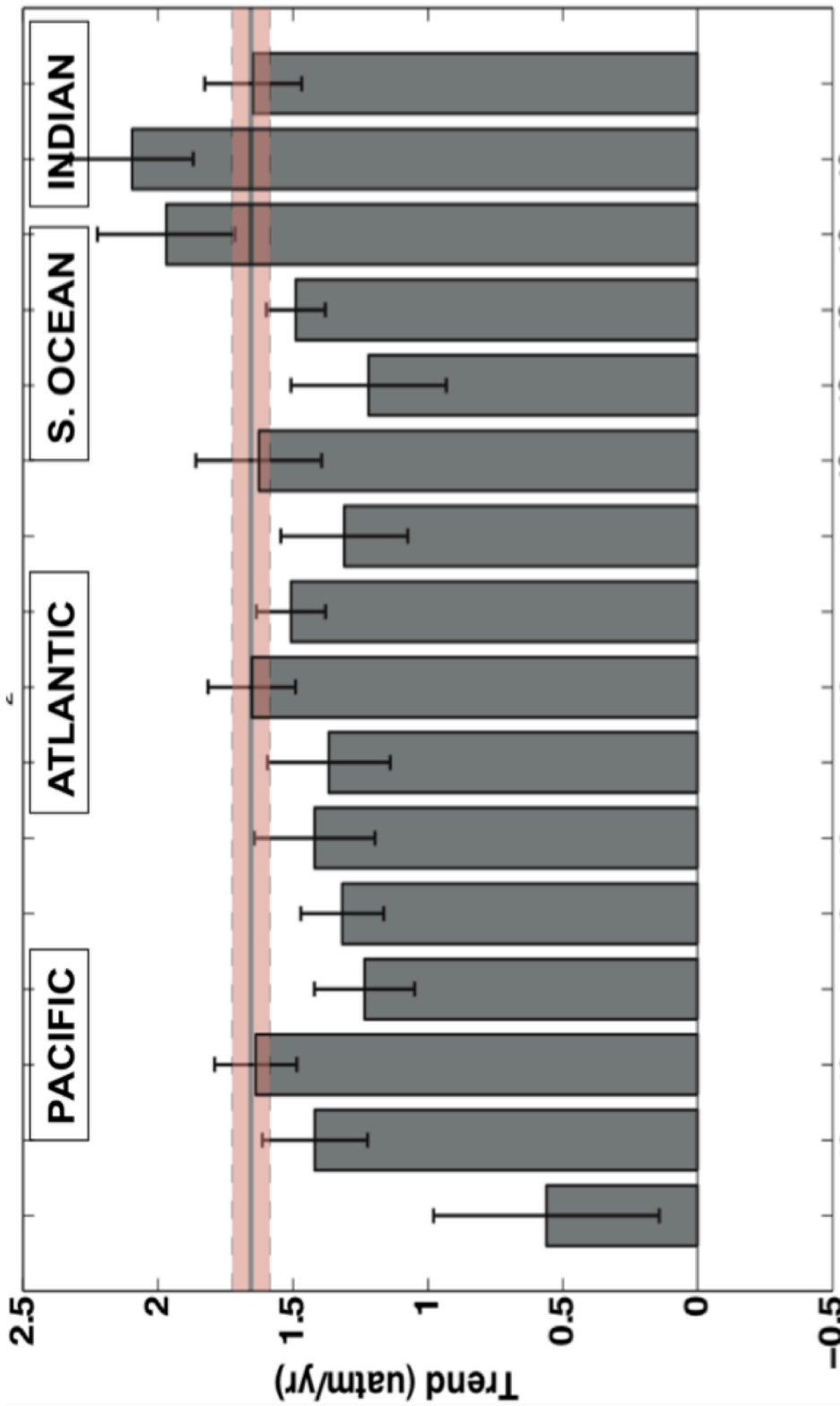

Figure 11. Bar plot showing trends in $pCO_2^{s.ocean}$ as compared to the atmospheric trend (represented by bold black line) for multi-decadal timescale (years 1981-2010). 1σ confidence intervals for each biome's $pCO_2^{s.ocean}$ trend is represented by the vertical errorbars while the 1σ CI for the atmospheric trend is represented by the pink shaded region

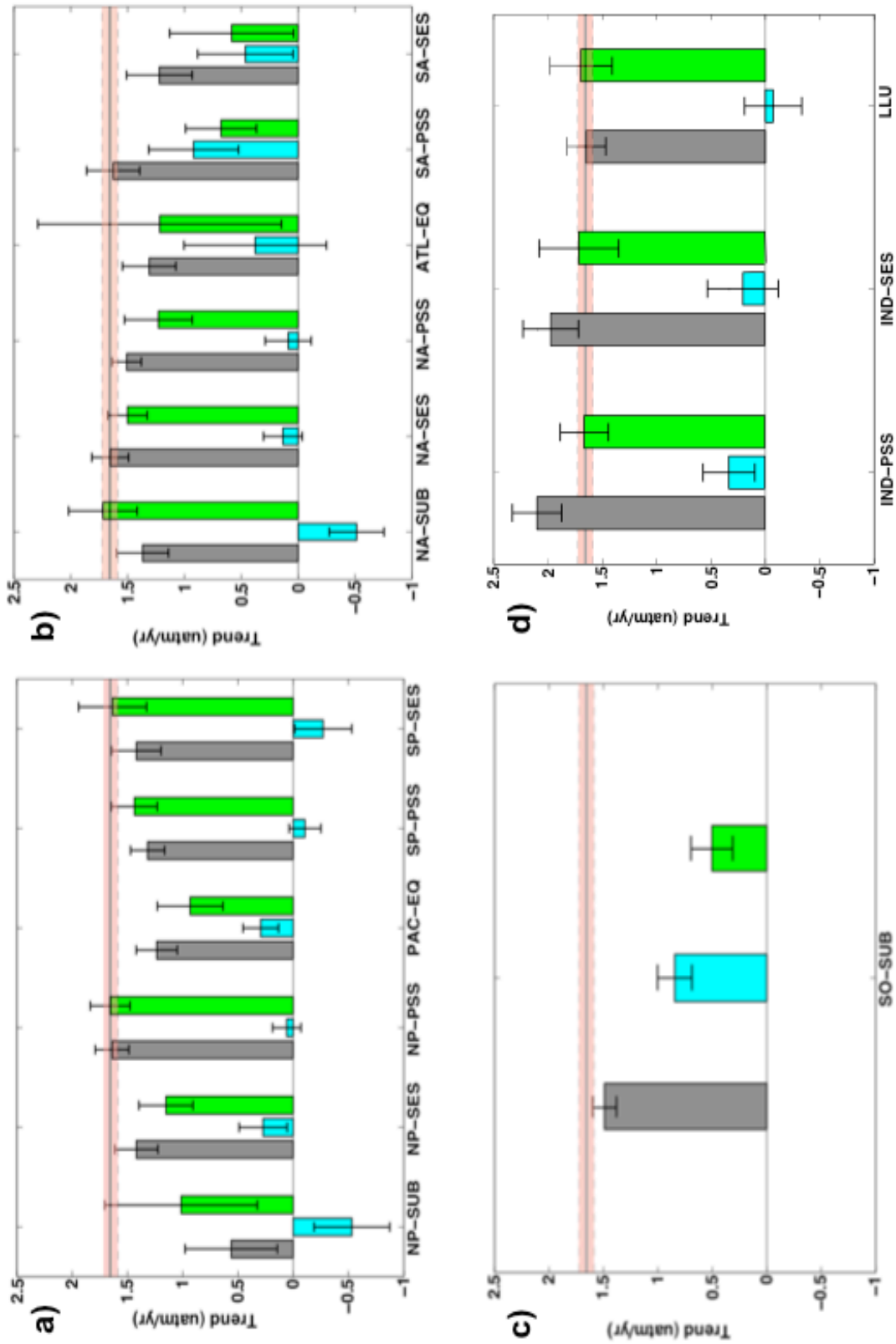

Figure 12. Decomposed pCO_2 trends for the multi-decadal timescale (1981-2010), separated by ocean basin. Gray bars represent $pCO_2^{s.ocean}$ trends, blue bars represent pCO_2-T components and green bars represent pCO_2-nonT components. As in Figure 11, the atmospheric trend and errorbars are included.

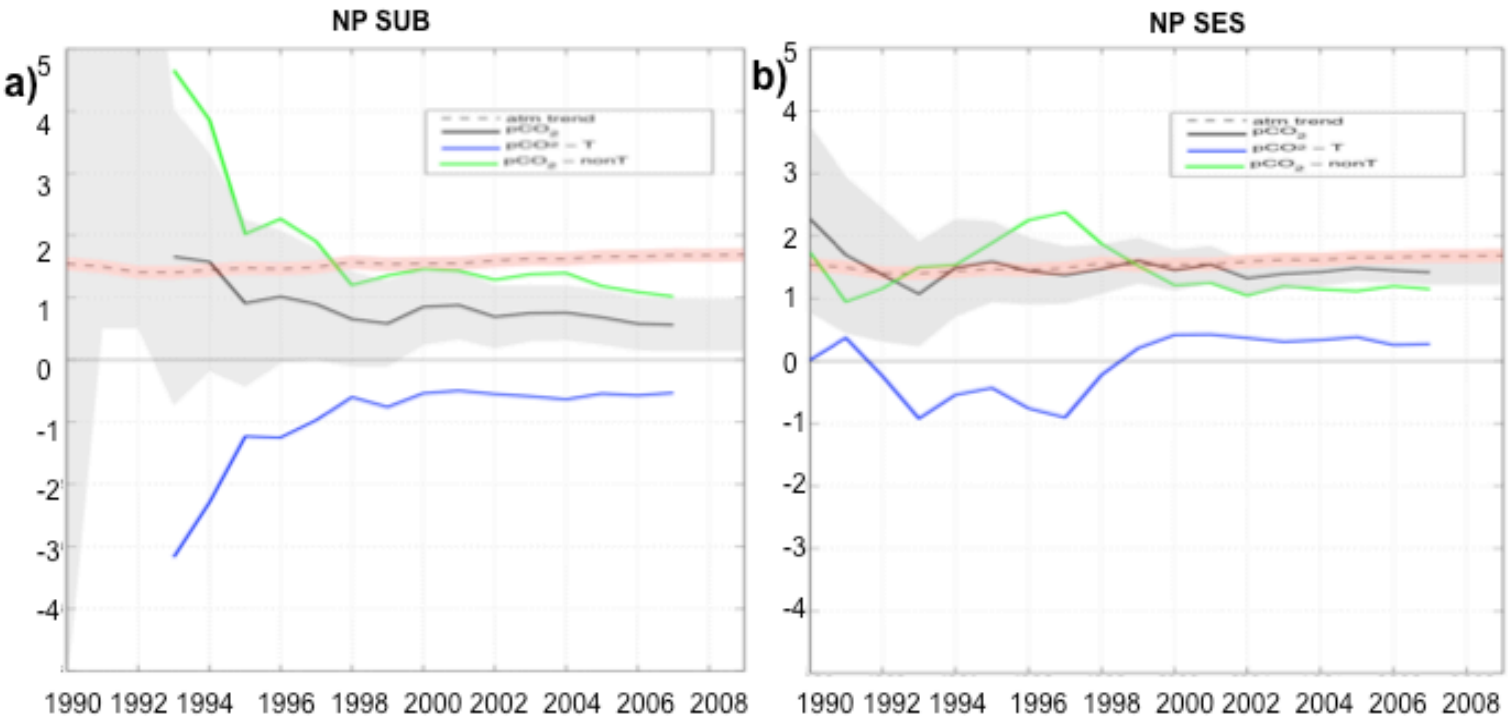

Figure 13. Plot of Pacific Ocean pCO_2 trends calculated beginning with 1981 through a changing end year (x-axis). The black line is the $pCO_2^{s.ocean}$ trend (gray shading is 1σ CI), dotted line and pink shading correspond to pCO_2^{atm}, green and blue lines represent pCO_2-nonT and pCO_2-T trends respectively.

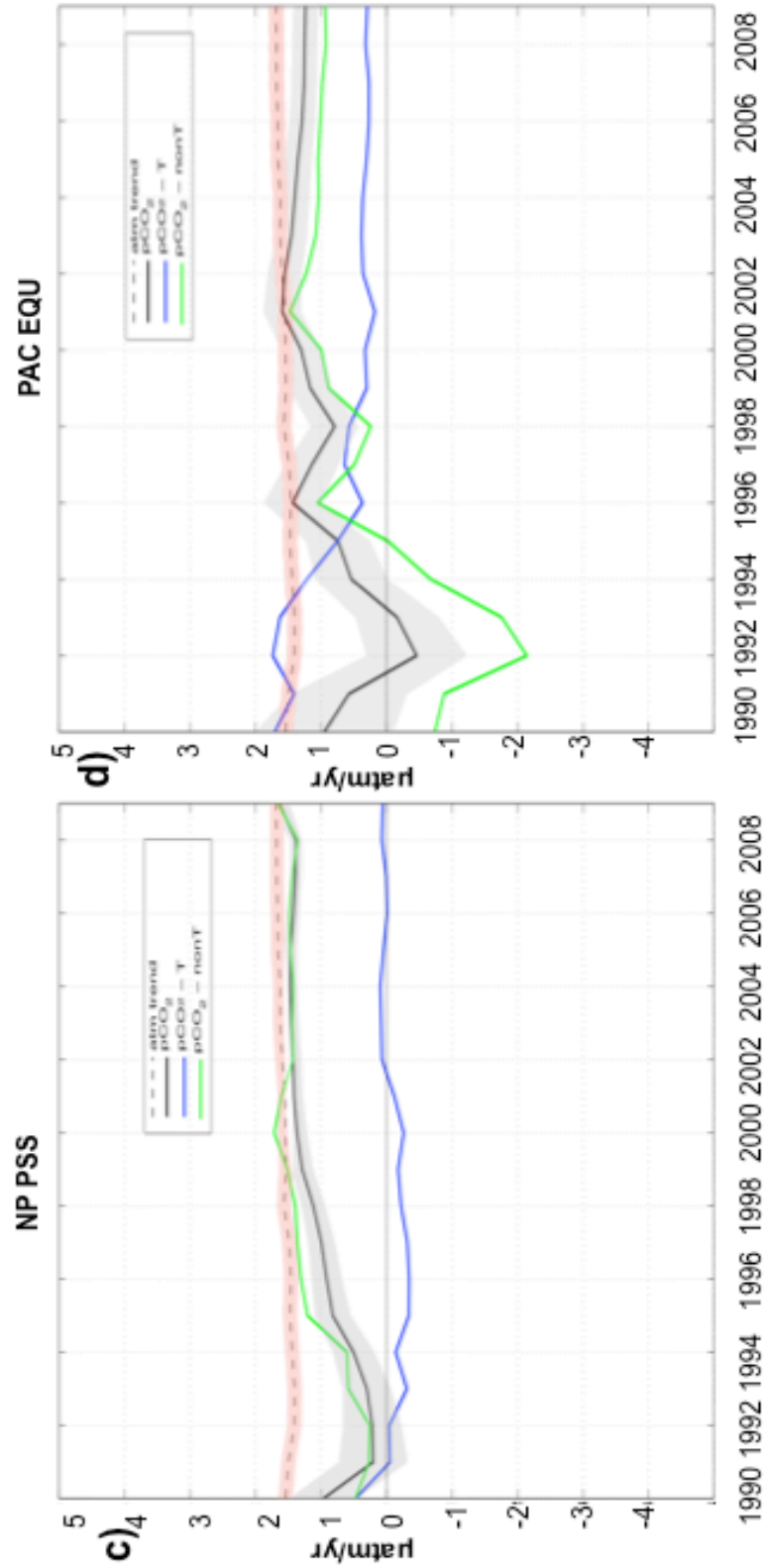
c)
NP PSS
d)
PAC EQU
µatm/yr
5
4
3
2
1
0
-1
-2
-3
-4
1990 1992 1994 1996 1998 2000 2002 2004 2006 2008
atm trend
pCO2
pCO2 – T
pCO2 – nonT

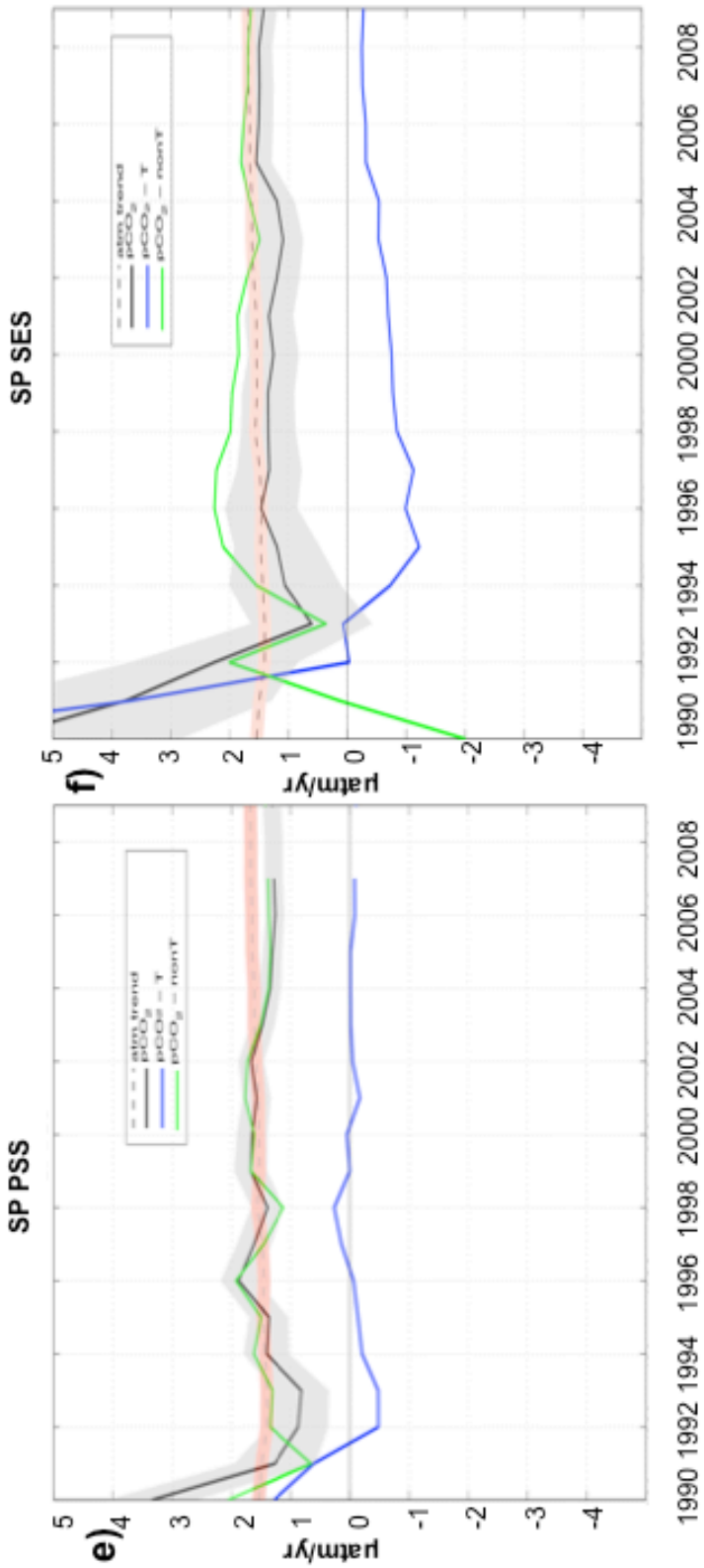
SP PSS
SP SES
e)
f)
patm/yr
1990 1992 1994 1996 1998 2000 2002 2004 2006 2008
5 4 3 2 1 0 -1 -2 -3 -4
atm trend
pCO2
pCO2 – T
pCO2 – nonT

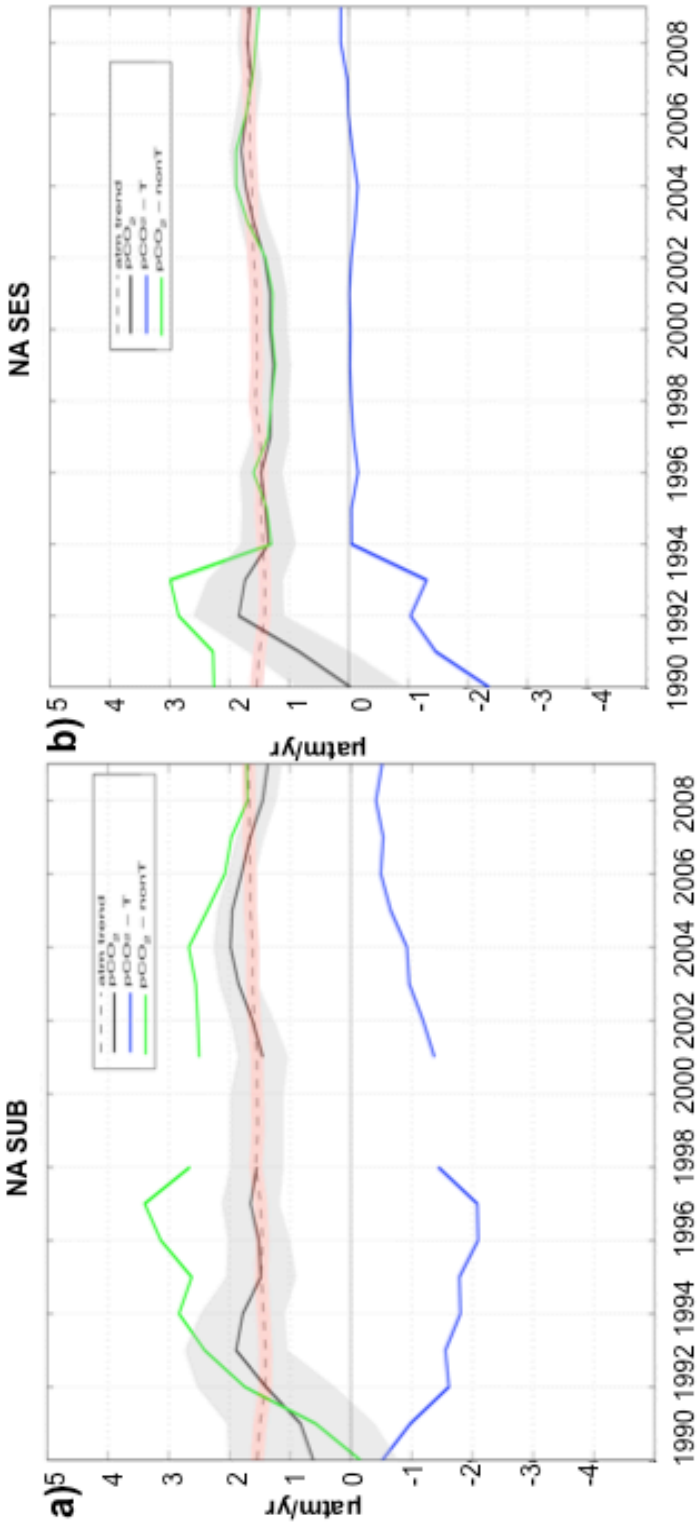

Figure 14. Plot of Atlantic Ocean pCO_2 trends calculated beginning with 1981 through a changing end year (x-axis). The black line is the $pCO_2^{s.ocean}$ trend (gray shading is 1σ CI), dotted line and pink shading correspond to pCO_2^{atm}, green and blue lines represent pCO_2-nonT and pCO_2-T trends respectively.

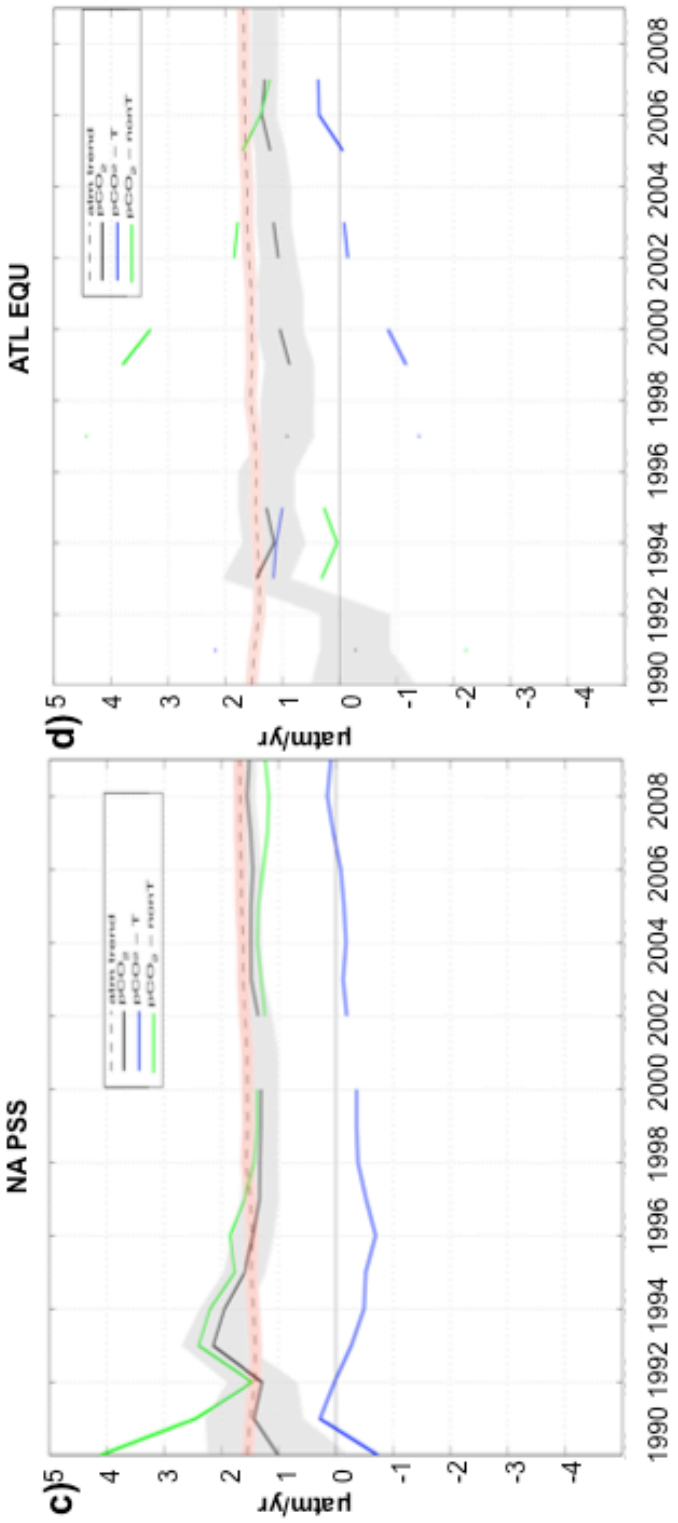
c)
NA PSS
d)
ATL EQU
µatm/yr
5
4
3
2
1
0
-1
-2
-3
-4
1990 1992 1994 1996 1998 2000 2002 2004 2006 2008
atm trend
pCO2 – T
pCO2 – nonT

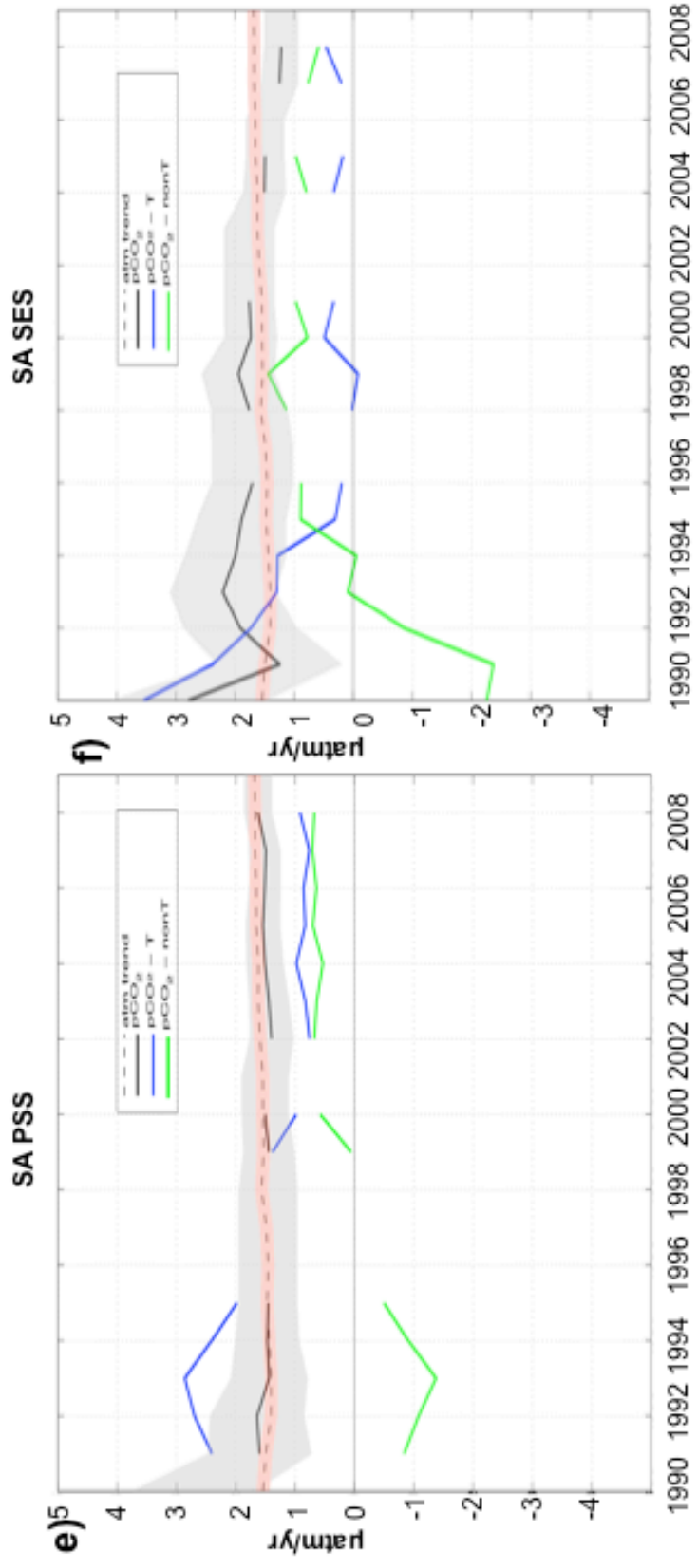
SA PSS
SA SES
e)
f)
μatm/yr
5
4
3
2
1
0
-1
-2
-3
-4
1990 1992 1994 1996 1998 2000 2002 2004 2006 2008
atm trend
pCO2 – T
pCO2 – nonT

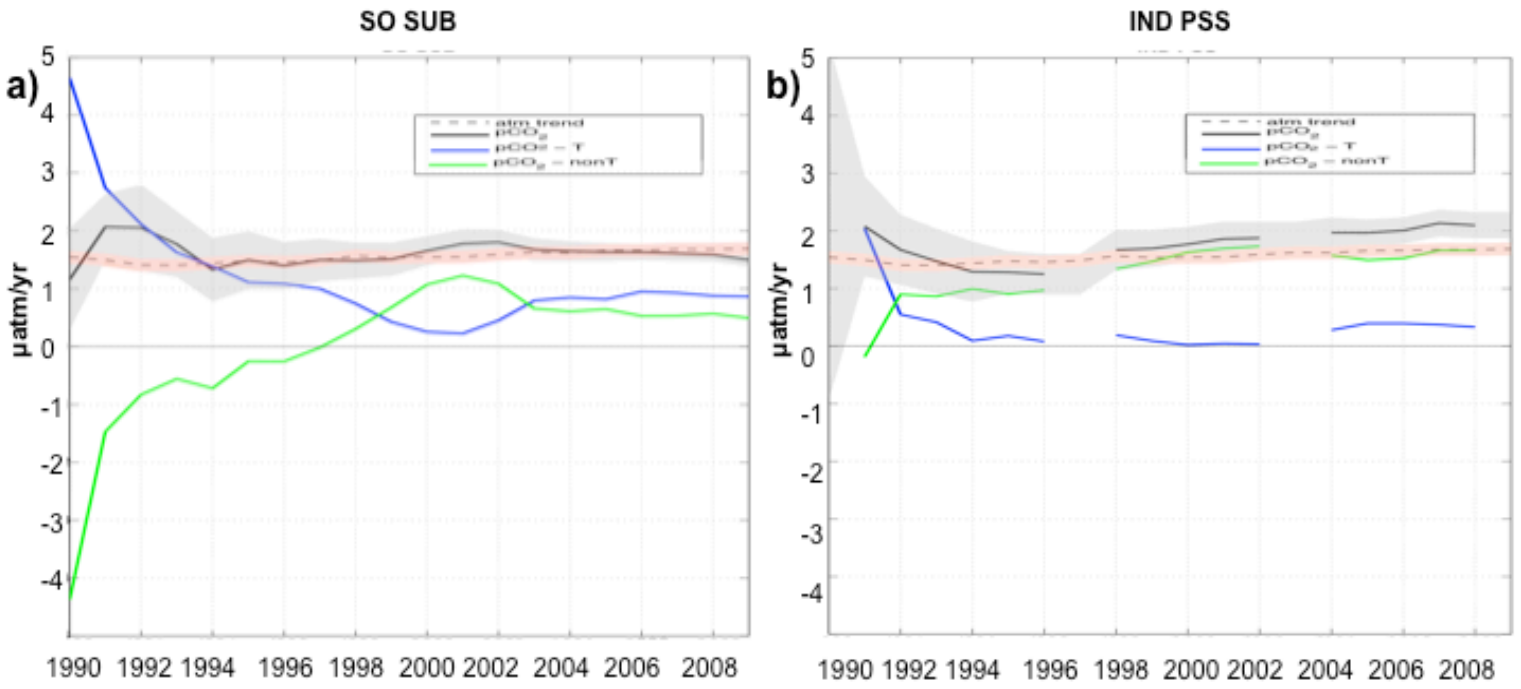

Figure 15. Plot of Southern Ocean and Indian Ocean pCO_2 trends calculated beginning with 1981 through a changing end year (x-axis). The black line is the $pCO_2^{s.ocean}$ trend (gray shading is 1σ CI), dotted line and pink shading correspond to pCO_2^{atm}, green and blue lines represent pCO_2-nonT and pCO_2-T trends respectively.

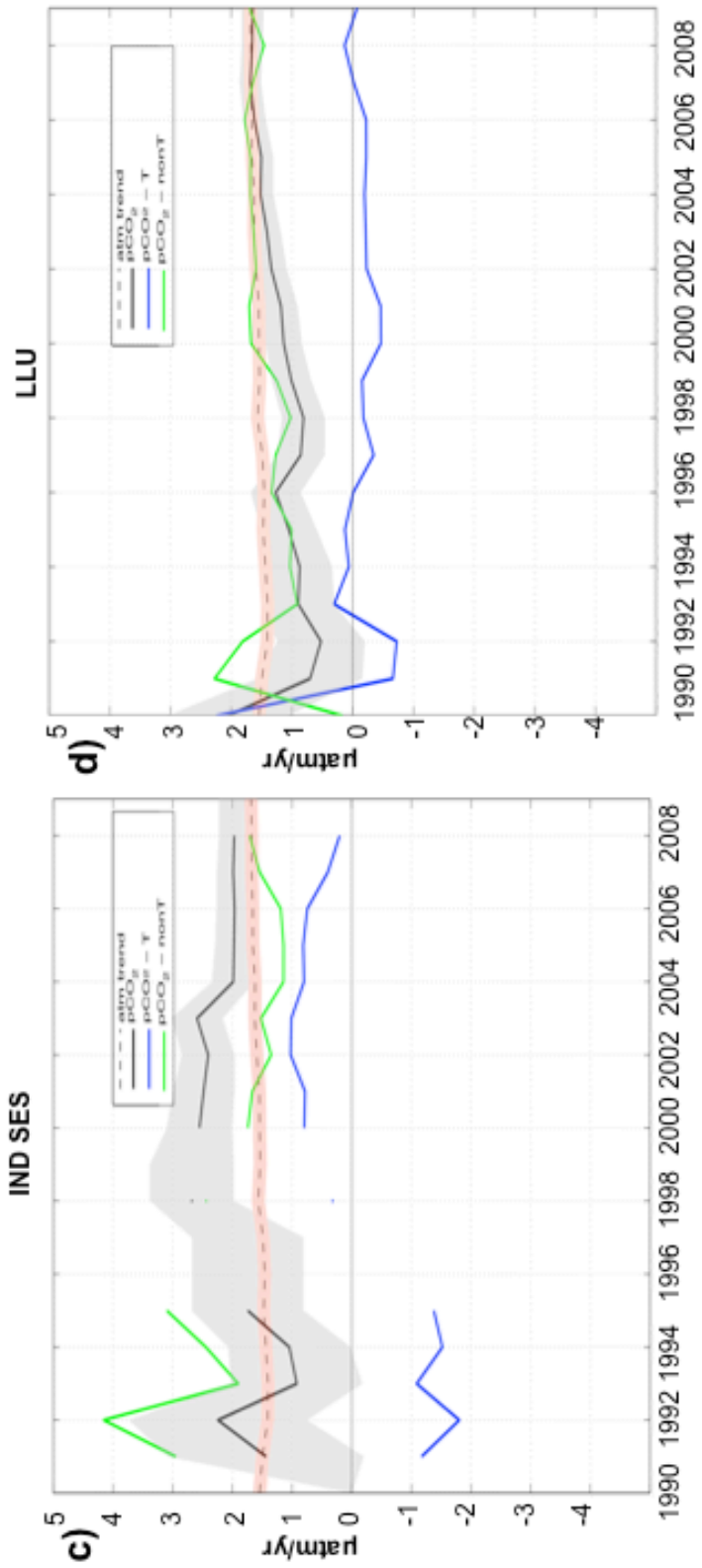
IND SES
LLU
c)
d)
μatm/yr
5
4
3
2
1
0
-1
-2
-3
-4
1990 1992 1994 1996 1998 2000 2002 2004 2006 2008
atm_trend
pCO_2
pCO_2 – T
pCO_2 – nonT